Monograph:
Hu, J.Q. and Rose, E. (1993) Simulation of an Iron Ore Sinter Plant. Research Report. ACSE Research Report 488 (b) . Department of Automatic Control and Systems Engineering

SIMULATION OF AN IRON ORE SINTER PLANT

J. Q. Hu and E. Rose

Department of Automatic Control & System Engineering
University of Sheffield
PO. Box 600 Mappin Street
Sheffield S1 4DU

Research Report No. 488 *(b)*

September 1993

SIMULATION OF AN IRON ORE SINTER PLANT

J. Q. Hu and E. Rose

Department of Automatic Control & System Engineering

University of Sheffield

September 1993

Abstract: This report refers to the work on the project " Parallel Distributed Method Applied to Control of a Sinter Plant". A review on modelling and simulation of a sinter bed is given here. The model consists of raw mixture preparation and sintering in the bed, the simulation includes heat exchange between solid and gas, water evaporation and condensing, limestone decomposition, coke consumption, gas flow, fusion of the mixture and solidification. The process state at any point of the bed can be calculated. The effect of changing process variables to sintering are investigated by running this simulation program. A dynamical simulation approach is proposed. The simulation algorithm described in this report will be used as a simulation model of the sintering process when investigating automatic control strategies for the sinter plant.

SINTERING PROCESS

Sintering is an important process in ironmaking. The required quality sinter is made from raw materials by means of the complex physicochemical reaction taking place during the process. A diagram of the sintering process is shown in Fig. 1. [1]

Preparation of Mixture

The raw materials used to prepare the mixture include iron-ore fines, fuel (normally coke breeze), return fines and limestone as flux. These raw materials are stored seperately in individual bins. The various materials are withdrawn from bins in certain proportions via weight belt feeders to ensure that the feed rate is maintained constant, and collected on a gathering belt. By this stage the primary chemical composition is formed.

The proportioned raw materials are next mixed and moistened, normally in two stages to provide a feed for the sinter strand having the correct physical texture. Firstly, in the primary mixing stage the raw materials are mixed with water and blended to ensure homogeneity. The bulk of the water addition should normally be made at this stage but this may be limited where the moistened mix becomes sticky, causing subsequent handling problems. The secondary mixing will basically complete the homogenization begun in the first mixing stage and will provide the rest of the water necessary to give the right physical texture to the mix; in this stage the moist mix is rolled to form pellets in a drum to give increased permeability. From the preparation of the mixture the chemical composition, the mean pellet diameter and the content of water in the mixture are determined; these will influence the sintering process.

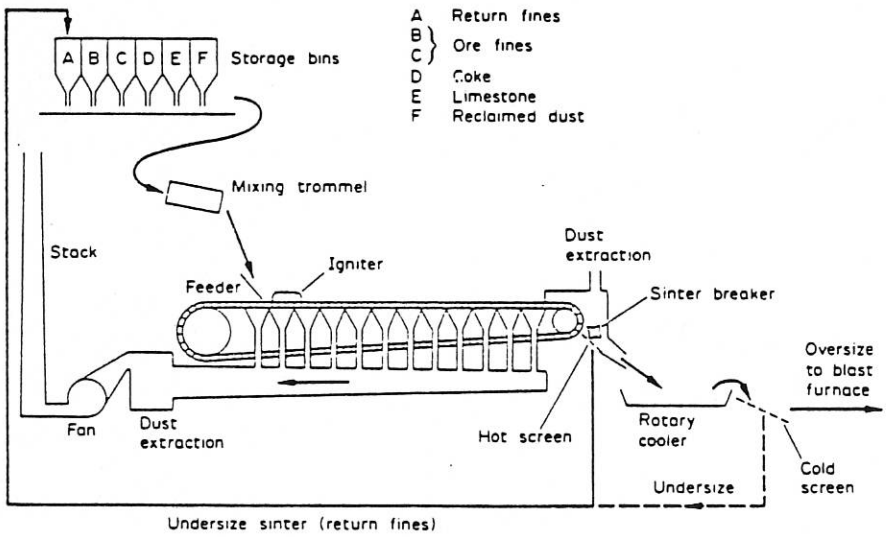

Fig. 1 General Arrangment of Sinter Plant

Sintering Process

The prepared mixture is now loaded onto a moving grate, the aim is to lay down the material evenly across the width of the strand. The feeding material is levelled by passing it under a cut-off plate fixed above the strand to form a flat bed of the required thickness, normally between 300 mm and 600mm. Next, the mix is ignited by means of a gas- or oil-burner mounted under an ignition hood. Ignition time and temperature play an important role during sintering process.

Thereafter sintering proceeds, air is sucked through the bed into windboxes situated under the grate and the strand moves forward at a speed of about 3 metres per minute. When the temperature of the top of the bed

reaches the burning point (about $770^{o}C$), coke combustion begins and due to the suction across the bed the heat-wave moves downward causing coke combustion through the bed. In an ideally steady process the combustion of coke at the bottom of the bed is completed and the solid temperature goes back to that below the melting temperature just before the sinter reaches the end of the strand[1].

The complex physicochemical reactions taking place during sintering include the following[2]:

(1) cooling: sintered material is cooled by cold air coming into the bed, the solid temperature decreased rapidly.

(2) cooling and solidification: after coke combustion has finished the melting heat is released gradually; partially melted material solidifies as the solid temperature reduces.

(3) coke combustion and fusion (melting): when the temperature of the solid material reaches melting temperature, most of the heat from coke combustion makes the mixture melt partially. The heat is stored in the form of latent heat and the solid temperature only rises slightly.

(4) heating and coke combustion: the temperature of the mixture rises rapidly along with coke combustion untill the solid temperature reaches the melting point.

(5) heating: the temperature of the bed rises due to the hot air drawn through it until the temperature reaches about $770C^{o}$.

(6) limestone reduction: limestone ($CaCO_3$) reduces to calcium (CaO) and carbon dioxide (CO_2), whilst the carbon dioxide content in the gas phase increases and the apparent density of the bed decreases. The temperature of solid rises gradually.

(7) drying: the water in the mixture is evaporated into gas and the bed temperature rises slowly.

(8) heating and condensing: the mixture is heated from its initial temperature to the point at which evaporation occurs. The moisture in gas is condensed into solid form when the solid temperature is below the dew point.

The heat-transfer and mass-transfer processes occur in a wide variety of ways. It is difficult to give a brief description of these processes, but in order to give some indication of all the major mechanisms likely to contribute, Fig. 2 shows a diagrammatic representation of the heat-transfer process and Fig. 3 shows a similar representation for the mass-transfer mechanism [3].

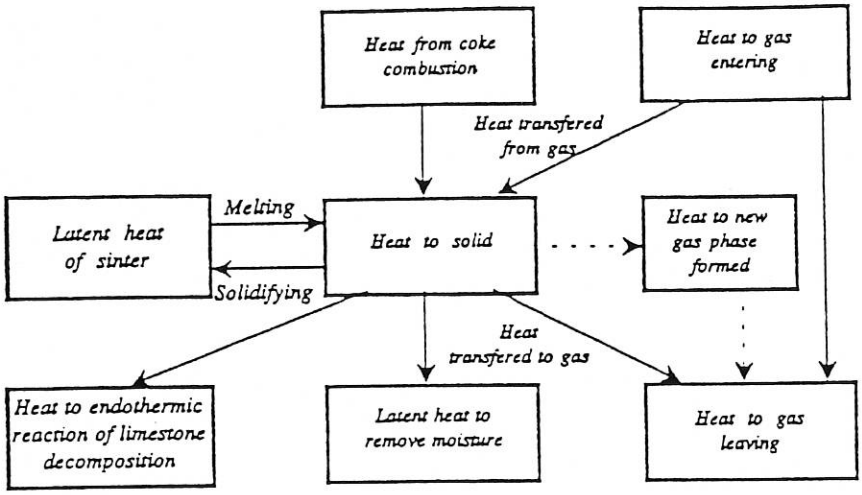

Fig. 2 Heat-transfer Process

The sintering product should achieve the required quality index which refers to chemical composition, mineral constituents, physical strength and reducibility.

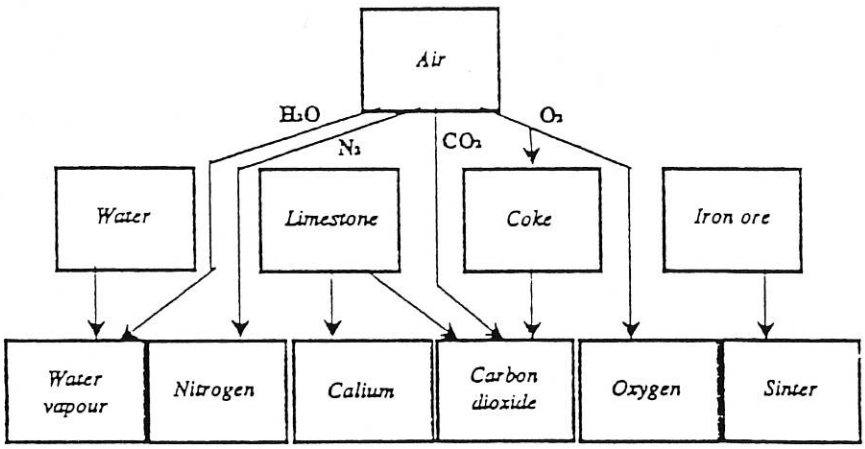

Fig. 3 Mass-transfer Process

PREVIOUS WORK ON MODELLING AND SIMULATION

Numerous mathematical models for the iron ore sinter bed process have been developed since 1970 and these have shown a progressive increase in refinement and an endeavour to optimise the process and its control. Each

was formulated as a series of differential equations describing the process at a point in the bed. These equations were solved numerically from the known initial condition in a vertical plane along the length of the sinter bed[4][5].

The first model of this type, which has served as a basis for many subsequent versions, is that of Muchi and Higuchi[6]; it principally takes into account heat transfer, coke combustion (Hottel's kinetic law) and drying, the influence of certain operating parameters was studied. Tukamoto et al.[7] added the description of limestone calcination and melting. Hamada et al.[8] added rate equations to describe the same phenomenon and show a qualitative agreement between the calculated result and measurement on a pilot pot. Yoshinaga and co-workers[9][10] developed a more extensive model; it included the feature of Hamada et al.'s model and, in addition, structural changes of the bed were modelled using different empirical factors for void-fraction and particle-diameter in each of three distinct zones. The presure drop across the bed was determined by applying the Ergun equation seperately across each zone and enabling good prediction of various quality criteria. Young[3] introduced a different calculation for the pressure drop and used a more sophisticated numerical method. Dash and Rose[11][12][13] considered drying at $100^{o}C$, condensing, melting at constant temperature, and a variable particle diameter. They improved the calculation of the gas flow and partially validated the calculation of the temperature. Nigo and co-workers[14][15] presented a model close to that of Muchi and Higuchi, but with a description of melting and of the change in porosity and particle diameter. They compared the temperature with those measured on three thermo-couples in the strand, and attempted to optimise the thermal profile using their model. Toda and Kato[16] developed a highly advanced model in terms of the physicochemical mechanisms considered, including the hematite magnetite reduction, different size of the coke particle and the melting kinetics, but do not mention the gas flow. The temperature and the percentage of FeO were compared with strand measurements and the water content to values determined on a pilot pot. Kasai et al.[17][18] developed a sophisicated model, but applicable to particular pellets (with alumina core), including numerous reaction, melting and solidification, together with a change in the porosity. However, a problem was encountered with the calculation of the maximium temperature attained by the solid. Cumming et al.[19] provide the most detailed model, describing a large number of physicochemical processes together with the variation of the bed characteristics (particle diameter, void fraction, tortuosity factor and shrinkage).

In the work described below, the approach used in this report is not intended to give an exhaustive description of all the physicochemical phenomena but follows the model developed by Rose and co-workers. The aim is to make the model as simple as possible with the condition remaining that the important physicochemical processes are faithfully represented.

MATHEMATICAL MODEL USED IN THIS REPORT

The model is based on the description of the real physicochemical and thermal mechanisms involved in the sintering operation. The aim of this study is to establish a simulation model and algorithm for automatic control strategies of the sintering plant. The adjustable input variables in the real sintering process are as follows: percentages of iron ore, return fines, coke addition, water addition and limestone addition, strand speed, height of the bed and the suction of the fan; these variables are used as inputs to model as well. The model is formulated as described below:

Preparation of The Mixture

The various raw materials are blended in this stage to form the chemical composition in the mixture and this chemical composition will affect the composition of the sintering product. The water is added to improve the permeability by pre-pelletizing the mixture and the physical properties of the mixture are determined initially in this stage as well.

The chemical composition of individual raw material is available from plant data, so the chemical composition of mixture can be obtained by a set of linear equations as follows:

$$C_i = \frac{\sum_{j=1}^{j=3} C_{ij} X_j}{\sum_{j=1}^{j=5} X_j} \tag{1}$$

where

C_i represents the i^{th} chemical composition in the mixture.

C_{ij} represents the i^{th} chemical composition in the j^{th} raw material.

X_j represents the addition of the j^{th} raw material.

The specific mass of initial mixture (including water addition) is determined by:

$$M_d = \frac{\sum_{j=1}^{j=4} X_j + X_w}{X_w + \frac{\sum_{j=1}^{j=4} \frac{X_j}{P_j}}{\sum_{j=1}^{j=4} X_j}} \tag{2}$$

where

P_j represents the specific mass of the j^{th} raw material.

X_1, X_2, X_3, and X_4 represent the additions of the iron-ore, return fines, limestone and coke respectively, X_w represents the addition of water.

The initial apparent density of the bed, the coke content of the bed, water content of the bed and limestone content of the bed are given by:

$$P_s = (1-\varepsilon)M_d \tag{3}$$

$$C_c = \frac{X_4 P_s}{\sum_{j=1}^{j=4} X_j + X_w} \tag{4}$$

$$C_w = \frac{X_w P_s}{\sum_{j=1}^{j=4} X_j + X_w} \tag{5}$$

$$C_l = \frac{X_3 P_s}{\sum_{j=1}^{j=4} X_j + X_w} \tag{6}$$

The initial mean pellet diameter is given by:

$$d_p = d + B_1 X_w \tag{7}$$

where d stands for mean particle diameter of the mixture, B_1 is the pelletizing constant.

Sintering Process

Because the physicochemical reaction occurring in the sintering process is too complex to give a detailed mathematical description of such a process, some assumptions must be made in modelling the process.

1. Gas flow is one-dimensional, vertical within the bed; there is no dispersion of gas within the bed because the gas travels through the bed in the vertical direction at a relative fast velocity.
2. The pressure drop is uniform from top to bottom of bed, and the suction from the fan is evenly distributed underneath strand.
3. There is no variation of solid or gas properties across the width of the bed.
4. The thermal conductivity within individual particles in the bed is infinitely high and the particles thus have a uniform temperature. Conduction between solid particles is negligible. Conduction in the gas

phase is low compare with convection, radiation is negligible so heat transfer occurs solely by forced convection which is the major factor promoting heat-wave propagation.

5. The reaction of coke and limestone particles start at the surface of the particles and take place at a definite moving boundary which leaves a core of unreacted material gradually shrinking with time.
6. In the combustion of coke only the $C + O_2 \longrightarrow CO_2$ reaction has been considered, and reduction of limestone occurs in the form of $CaCO_3 \longrightarrow CaO + CO_2$.
7. The solid temperature cannot rise until the moisture has been evaporated completely and the solid temperature does not rise too much when the solid temperature reaches the melting temperature.

It follows from these assumptions that there is no heat or mass transfer from the solid of the bed or gas phase in a lateral direction within the bed, so all state variables are invariant with the lateral coordinate throughout the bed. The mathematical description of the sintering process can be formulated in the following differential equations based on a very small part within the bed regarded as a point.

Thermal energy balance equation for the gas phase:

$$u\varepsilon\frac{\partial(C_g P_g t_g)}{\partial x} + \varepsilon\frac{\partial(C_g P_g t_g)}{\partial t} = ah_p(t_s - t_g) \tag{8}$$

where

u gas velocity passing through the point to which equation refers, m/s.

ε the bed voidage (= volume of voids / specific volume of material).

x refer to the depth that the point goes into the bed from the top surface of the bed, m.

t refer to the time, s.

t_g standing for gas temperature, it is the function of the depth x and time t. i.e $t_g = f_1(x, t)$, K.

t_s standing for solid temperature, it is the function of time t only, i.e $t_s = f_2(t)$, K.

C_g specific heat of gases, $J/Kg.K$. subject to $C_g = 880.0 + 0.31t_g - 8.0\times10^{-5}t_g^2$

P_g density of gas mixture, Kg/m^3. subject to $P_g = (32C_{o_2} + 44C_{co_2} + 28C_{N_2} + 18C_{H_2O})10^{-3}(273/t_g)$

a specific solid area per unit volume of bed, m^2/m^3. subject to $a = 6(1-\varepsilon)/d_p$. Here d_p standing for mean pellet diameter of mixture, m.

h_p convective heat transfer coefficient between solid particles and gas, J/m^2sK.

Molar balance equations for the components of gas phase:

$$u\varepsilon\frac{\partial C_{o_2}}{\partial x} + \varepsilon\frac{\partial C_{o_2}}{\partial t} = -R_c \tag{9}$$

$$u\varepsilon\frac{\partial C_{co_2}}{\partial x} + \varepsilon\frac{\partial C_{co_2}}{\partial t} = R_c + R_l \tag{10}$$

$$u\varepsilon\frac{\partial C_{H_2O}}{\partial x} + \varepsilon\frac{\partial C_{H_2O}}{\partial t} = \frac{R_H}{M_{H_2O}} \tag{11}$$

where

C_{O_2}, C_{CO_2} and C_{H_2O} are the malor concentration of species oxygen (O_2), carbon dioxide (CO_2), and water (H_2O) respectively in gas phase, mol/m^3.

R_c, and R_l are reaction rate of coke (in the form of $C + O_2 \longrightarrow CO_2$) and limestone (in the form of $CaCO_3 \longrightarrow Ca + CO_2$) respectively, mol/m^3s.

R_H is the transfer rate of moisture from solid phase to gas phase (or reversed), Kg/m^3s.

The vertical passage of the gas through the bed is so fast that the dynamics of change of its state variables with time need not to be considered[4] so the equations (8)(9)(10)(11) are reduced to the normal differential equations as follows:

$$u\varepsilon\frac{\partial(C_g P_g t_g)}{\partial x} = ah_p(t_s - t_g) \tag{12}$$

$$u\varepsilon\frac{\partial C_{o_2}}{\partial x} = -R_c \tag{13}$$

$$u\varepsilon\frac{\partial C_{co_2}}{\partial x} = R_c + R_l \tag{14}$$

$$u\varepsilon\frac{\partial C_{H_2O}}{\partial x} = R_H \tag{15}$$

Thermal energy balance equation for the solid:

$$\frac{\partial(P_s C_s t_s)}{\partial t} = ah_p(t_g - t_s) + H_c R_c + Q_a \tag{16}$$

where

P_s apparent density of the bed, K_g/m^3.

C_s specific heat of mixture in th bed, J/KgK. subject to $C_s = 753.0 + 0.25t_s$.

H_c heat of combustion of coke, J/mol, equal to 2.953×10^5 in this report.

Q_a additional heat to the bed (or from the bed) by water evaporating or condensing, limestone decomposition and mixture melting or solidifying, which depends on the zone where the considered point is, J/m^3s.

Total mass balance of solid phase:

$$\frac{dP_s}{dt} = \left(\frac{d\rho_c}{dt} + \frac{d\rho_{H_2O}}{dt} + \frac{d\rho_l}{dt}\right) \tag{17}$$

Carbon mass balance of sold phase:

$$\frac{d\rho_c}{dt} = -M_c R_c \tag{18}$$

Water mass balance of solid phase:

$$\frac{d\rho_{H_2O}}{dt} = -M_{H_2O} R_H \tag{19}$$

Limestone mass balance of solid phase:

$$\frac{d\rho_l}{dt} = -M_{co_2} R_l \tag{20}$$

where

M_c, M_{H_2O} and M_{co_2} stand for molar mass of carbon, water and carbon dioxide respectively, Kg/mol.

ρ_c, ρ_{H_2O} and ρ_l are the contents of coke, water and limestone in the mixture, Kg/m^3. Their initial values are obtained by equ. (4) to equ. (6).

Equations Related with Rates and Coefficients

The gas velocity in the bed u:

the gas travels through the bed due to the suction of the fan. The gas flow rate (velocity) can be determined by the physical property of the bed, and the suction, regarded as an input variables to the process, is used to calculate a desired pressure drop across the bed. Suppose that the suction of the fan is represented as ΔP, the effective area of the bed is A, and the thickness of the bed is h then the presure drop through the bed is given in the vertical direction of the bed:

$$\frac{dp(x)}{dx} = -\frac{\Delta P}{Ah} \tag{21}$$

By using Ergun's equation in the differential form, the gas velocity is calculated throughout the bed:

$$-\frac{dp(x)}{dx} = 150\frac{(1-\varepsilon)^2}{\varepsilon^3 d_p^2}\mu u + 1.75\frac{1-\varepsilon}{\varepsilon^2 d_p}P_g u^2 \tag{22}$$

where

μ stand for the viscosity of the gas, Kg/sm, which is calculated by:

$$\mu = \mu_0\left(\frac{t_g}{273}\right)^{3/2}\frac{C + 273}{C + t_g} \tag{23}$$

μ_0 is the viscosity at 0^oC and C is a constant, the value of which depends on the gas type.

The coefficient of convectivity h_p:

it depends upon the physical properties of the solid and gas. The formulation of the heat transfer coefficient is based on the following relationship between the Nusselt, Reynolds and prandtl numbers Nu, Re and Pr respectively:

$$N_u \varepsilon = F(P_r, R_e) \tag{24}$$

where

$N_u = h_p d_p/\lambda$, $R_e = d_p u \varepsilon P_g/\mu$ and $P_r = C_g/\lambda$.

λ is the thermal conductivity of the gas, J/smK. subject to $\lambda = 0.012 + 5.14\times10^{-5} t_g$.

For a sinter bed it is considered[6] that the most appropriate equation is:

$$N_u \varepsilon = 2.0 + 0.71 P_r^{1/3} R_e^{1/2} \tag{25}$$

so the coefficient of convectivity h_p is given:

$$h_p = N_u \lambda / d_p = \frac{\lambda}{\varepsilon d_p}(2.0 + 0.71 P_r^{1/3} R_e^{1/2}) \tag{26}$$

Reaction rate of coke R_c (for coke combustion) $mol/m^3 s$:

the overall combustion of coke particles is dependent upon both chemical and mass transfer because, before combustion of coke can occur, oxygen has to diffuse to the surface of the coke particles. The overall combustion rate R_c is given by the equation:

$$R_c = 4\pi r_c^2 N_c K C_{o_2} \tag{27}$$

where

$4\pi r_c^2$ is the surface area of a coke particle (suppose that the coke particles exist in the form of micropellet).

N_c is the number of coke particles per unit volume of bed.

K_m is the coefficient of mass transfer.

K_c is the chemical combustion rate constant.

$$K = K_c K_{ml}/(K_c + K_{ml})$$

A formula exists for the coefficient of mass transfer between the gas and particles, which is similar to the coefficient of thermal convectivity:

$$S_h \varepsilon = 2.0 + 0.71 S_c^{1/3} R_e^{1/2} \tag{28}$$

where $S_h = K_m d_p / D$, $S_c = \mu / P_g D$.

D stands for the diffusion coefficient. The value of the diffusion coefficient of oxygen through nitrogen D_{ON} is given by Parker and Hottel[20]:

$$D_{ON} = 1.8\times10^{-5}(\frac{t_g}{273})^{3/2} \tag{29}$$

therefore the coefficient of mass transfer K_{ml} is given by:

$$K_{ml} = \frac{D_{ON}}{d_p \varepsilon}(2.0 + 0.71 S_c^{1/3} R_e^{1/2}) \tag{30}$$

Parker and Hottel[20] gave the following formula for the chemical combustion rate K_c as well:

$$K_c = 6.52\times10^5 e^{-18500/Rt_s}\sqrt{t_s} \tag{31}$$

The number of coke particles per unit volume is calculated by the following formula initially and keep constant during the process proceeding:

$$N_c = \frac{C_c}{\frac{4}{3}\pi r_{0c}^3 P_c} \tag{32}$$

where

X_4 is the addition of coke in mixtuer

P_c is the density of coke, Kg/m^3.

r_{0c} is the initial radius of coke particles, m.

The radius of a coke particle r_c changes its size along with the coke combustion, the rate is:

$$\frac{dr_c}{dt} = \frac{-12\times10^{-3}KC_{o_2}}{P_c} \tag{33}$$

according to a shrinking-core model described by Schulter and Bistranes[21].

The limestone reaction rate R_l (for limestone decomposition), mol/m^3s:

when the solid temperature reaches about 600^oC limestone decomposition occurs, C_aCO_3 in limestone reduces to C_aO and CO_2 at the rate R_l which is given by:

$$R_l = \frac{Q_f}{H_l} \tag{34}$$

where

Q_f total heat available for limestone decomposition from bed, J/m^3s.

H_l specific heat for limestone decomposition, J/mol, is taken as 1.890×10^5 in this report.

Evaporating (or condensing) rate of moisture R_h, mol/m^3s:

which is formulated according to the assumption that evaporation happens when solid temperature reaches at 100^oC and the solid temperature stays constant at 100^oC during evaporation, condensation exists when the gas temperature goes down to dew-point 60^oC and the gas temperature keeps its temperature constant during condensing.

$$R_h = \frac{Q_w}{H_w} \tag{35}$$

where

Q_w total heat available for moisture evaporation from bed or for moisture condensing to bed.

H_w latent heat for evaporation for condensing, J/Kg, equal to 2.290×10^6 in this report.

Melting and Solidification

The heat produced from the coke combustion causes the temperature to rise to a value in the range $1200^{o}C - 1400^{o}C$ and bonding takes place between the particles. Analytical modelling of the fusion phase is extremely complex; Dash and Rose presented an approach to consider the fusion which is to allow the temperature to rise to a prescribed value (in the range of $1200^{o}C - 1400^{o}C$) and to store the excess heat, assuming it to be used in fusion, until the cool air drawn through the bed behind the combustion zone causes the temperature to drop.

Sato et. al.[23] developed a melting model for iron ore sintering which takes account of the mix chemical composition. The model uses the proportion of CaO, Al_2O_3 and SiO_2, (the major slag forming components of the mixture) to calculate the temperature at which the mix begins to melt. Combining these approaches the mathematical description is formulated for melting and solidification. Mean pellet diameter is allowed to increase along with melting.

Critical melting temperature T:

$$T = 1106 - 3.19CaO - 3.35SiO_2 + 21.22Al_2O_3 \tag{36}$$

where CaO, Al_2O_3 and SiO_2 are the percentage fraction of these components in the mixture.

Melting occurs when the solid temperature reaches the critical melting temperature T the particles begin to melt. Most of the heat obtained by solid is to be used for melting and to be stored as latent heat; the solid temperature rises slowly. The melting heat is calculated by the equation:

$$\frac{dQ_f}{dt} = F_m \times Q \tag{37}$$

where

Q_f is the latent heat of melting, J.

F_m is the melting heat fraction.

Q is the total heat obtained by solid without considering melting, J/m^3s.

The melting fraction F_m can be determined by:

$$F_{ml} = \frac{t_{sml} - T_G}{t_{sml} - T} \tag{38}$$

where

t_{sm} stands for the maximium temperature which the bed can reach without melting.

T_G stands for the maximium temperature which the bed can reach with melting, subject to $T_G = 1306 - 3.19CaO - 3.35SiO_2 + 21.22Al_2O_3$.

Sato et. al. used their model to calculate what they term the melt fraction index f which is shown to be directly related to sinter strength. The melt fraction index is given by:

$$f = \sum_j [\, 1 - (1 - 2v_j\tau / d_j)^3]\, X_j \tag{39}$$

where

τ is the melting time above the melt-up temperature, s.

d_j is the particle diameter of the j^{th} mix constituent, m.

X_j is the percentage of the j^{th} mix constituent.

v_j is the melting rate of the j^{th} mix constituent, m/s, which is given by:

$$v_j = 1.67\times10^{-5}(0.0147\varepsilon_j - 0.09) \tag{40}$$

here ε_j is the dry porosity of the j^{th} mix constituent, this is not the same as the bed voidage it is the voidage within the particles before pelletizing.

Solidification occurs when the combustion of coke has finished, no extra heat is supplied to the bed except the latent heat stored in the melted part of particles is released. This is found by using the equation:

$$\frac{dQ_f}{dt} = F \times Q_1 \tag{41}$$

where Q_1 is the required heat by heat transfer between the solid and gas in the bed, J/m^3s, until the latent heat does not exist any more.

The heat released as latent heat serves to heat the cold air coming into the bed. This results in the solid temperature decreasing slowly.

Mean pellet diameter is increased gradually at an increasing rate due to the mixture melting, given by:

$$\frac{d\ d_p}{dt} = B \tag{42}$$

where B stands for the increasing rate. We will assume B is constant and determined by the initial mean pellet diameter and final mean pellet diameter.

SIMULATING THE SINTER PLANT

During sintering a number of processes occur simultaneously in the bed. In a partially sintered bed the material at the top consists of cooling sinter whilst the bottom of the bed may be unprocessed. There exist therefore a number of regions in which different processes are proceeding.

A typical bed-temperature profile of a section in the bed is shown in Fig. 4, on which the different regions are marked.

In order to obtain the digital solution for the equations described in the above section the bed is assumed to be divided vertically into n zones, and horizontally into m sections (Fig.5) along with strand.

The thickness of the i^{th} zone is Δx_i and therefore $\sum_{i=1}^{i=n} \Delta x_i = h$, where h is the thickness of the whole bed. The width of the j^{th} section is Δl_j and $\sum_{j=1}^{j=m} \Delta l_j = L$, where L is the length of the strand. The time that the bed travels through a section is determined by $\Delta t = \Delta l_j / v$, where v is the strand speed. Considering the ignition hood fixed above the strand occupying the length L_{in}, the ignition period will be L_{in}/v

Anderson's work[23] indicated that the digital solution to a continous sintering process converges when the thickness of a zone and the width of a section are reduced to $3mm$ and $2s$ respectively. Therefore the thickness of a zone is selected to be $3mm$, the time by which the bed travels through a section is to be less than $2s$ (which is equivalent to the minimium strand speed $2.4\ m/min$ if the strand is divided into 1000 sections and the length of strand is regarded as $80\ m$ long).

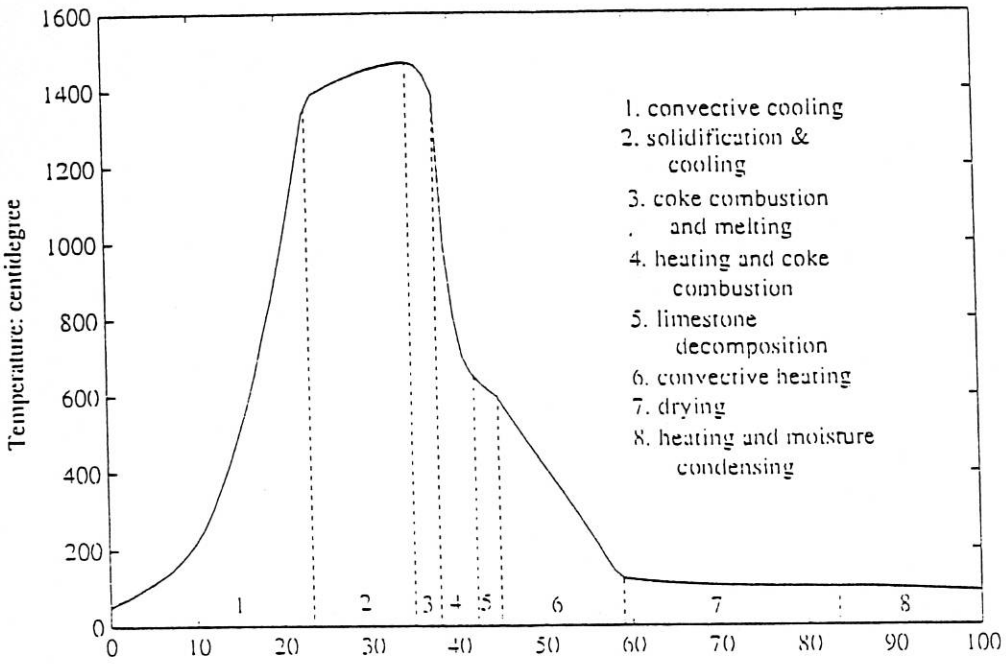

Fig. 4 Temperature Profile Showing Process Phase

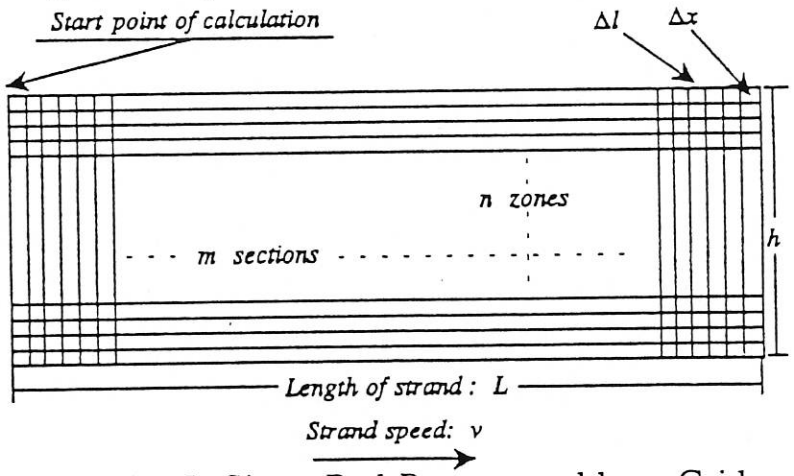

Fig. 5 Sinter Bed Represented by a Grid

Basic Method

The simulation method is best described initially for the case of pure convective heat transfer between the solid and gas, neglecting the phase representing drying, combustion, fusion and limestone reduction. Consider a narrow band of gas of thickness δx, ($\delta x \ll \Delta x_i$) passing downward through each zone of the bed in turn at the gas velocity u entering the i^{th} zone at temperature $t_g(i,j)$ and leaving the i^{th} zone at temperature $t_g(i+1,j)$. Because of the large difference in density between the solid and the gas (approximately 3000:1 [2]), it is admissible to allow the solid temperature $t_s(1)$ .....

$t_s(n)$ in the zone 1 to n respectively to remain constant while the narrow gas band is passing through it for a prescribed period Δt (which greatly exceeds the time taken for the band of gas to make one pass through the zone of bed). By this way the gas temperature profile is calculated in a section of bed. Meanwhile consider a narrow band of solid material of width δl ($\delta l \ll \Delta l_j$) moving forward through each section of the bed sequentially at the strand speed v with temperature $t_s(i,j)$ (where i refers to the i^{th} zone) entering the j^{th} section and leaving it at the temperature $t_s(i,j+1)$. It is also admissible to allow the gas temperature $t_g(1)$ ..... $t_g(n)$ in zones 1 to n respectively to remain at the value obtained from the previous calculation for a period Δt; in this way the solid temperature is updated after a time interval Δt. The complete solution is carried out on a depth-time plane, Fig. 6 shows the procedure of calculating gas and solid temperature in such a plane, where the solutions are generated at the vertices of the rectangular grid. Each vertical arrow represents digital solution of the gas equation (11) over a depth interval Δx, and each horizontal arrow represents the updating of the solid temperature over a time interval Δt, i.e a length interval of the strand Δl.

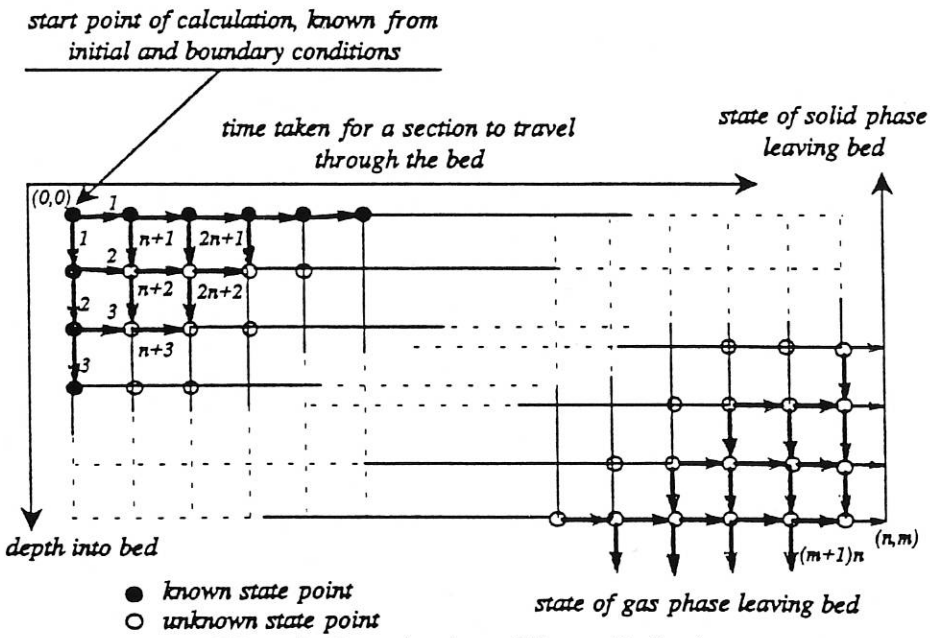

Fig. 6 Depth-time Plane Solution

Although the gas temperature is defined as a function of depth of bed x and the solid temperature as a function of time t, both variables t_g and t_s have different distributions in the individual zone and section respectively so they are groups of functions defined as follows:

$$t_{g_j} = t_g(x, j) \tag{43}$$

$$t_{s_i} = t_s(i, t) \tag{44}$$

where i represents the i^{th} zone and j represents the j^{th} section in the depth-time plane.

The equations (12),(16) are given in the discrete form as follows (note that equation (16) is reduced to the form of representing convective heat transfer only):

$$t_g(i+1, j) = t_g(i, j) + \frac{\Delta x a h_p(i, j)}{u \varepsilon P_g(i, j) C_g(i, j)} [t_s(i, j) - t_g(i, j)] \tag{45}$$

$$t_s(i, j+1) = t_s(i, j) + \frac{\Delta t a h_p}{P_s C_s(i, j)} [t_g(i, j) - t_s(i, j)] \tag{46}$$

where

$$P_g(i, j) = (32C_{O_2} + 44C_{CO_2} + 28C_{N_2} + 18C_{H_2O}) 273 \times 10^{-3} / t_g(i, j) \tag{47}$$

$$C_g(i, j) = 880.0 + 0.31 t_g(i, j) - 8.0 \times 10^{-5} t_g^2(i, j) \tag{48}$$

$$C_s(i, j) = 753.0 + 0.25 t_s(i, j) \tag{49}$$

$$h_p(i, j) = \frac{\lambda(i, j)}{\varepsilon d_p} (2.0 + 0.71 P_r^{1/3}(i, j) R_e^{1/2}(i, j)) \tag{50}$$

$$\lambda = 0.012 + 5.14 \times 10^{-5} t_g(i, j) \tag{51}$$

$$P_r = C_g(i, j) / \lambda(i, j) \tag{52}$$

$$R_e = d_p u \varepsilon P_g(i, j) / \mu(i, j) \tag{53}$$

$$\mu(i,j) = \mu_0\left(\frac{t_g(i,j)}{273}\right)^{3/2}\frac{C + 273}{C + t_g(i,j)} \qquad (54)$$

It is shown that the value of the process state variables at the upper left corner of each square in the depth-time plane determines the vertical change in gas temperature and the horizontal change in solid temperature by convective heat transfer between gas and solid from equations (45) and (46). Given a set of initial values and boundary conditions are as follows:

initial solid temperature	$t_s(i,0) = 25^o C$	$i=0,\ldots\ldots,n$
gas temperature for ignition	$t_g(0,j) = 1180^o C$	$j=0,\ldots\ldots,L_h$
gas temperature after ignition	$t_g(0,j) = 25^o C$	$j=L_h+1,\ldots\ldots,m$
suction of the fan	$\Delta P = 600000\ Kg\ m\ /\ s^2$	
strand speed	$v = 4.2\ m\ /\ \min$	
oxygen content in gas	$C_{O_2} = 20\ \%$	
carbon dioxide content in gas	$C_{CO_2} = 0.0\ \%$	
nitrogen content in gas	$C_{N_2} = 80\ \%$	
limestone addition in mixture	$X_3 = 0.0\ \%$	
coke addition in mixture	$X_4 = 0.0\ \%$	
water addition in mixture	$X_w = 0.0\ \%$	
mean pellet diameter	$d_p = 10\ mm$	

and given the following constants:

length of strand	$L = 80\ m$
width of strand	$W = 4\ m$
height of bed	$h = 300\ mm$
ignition period	$L_h = 100$
voidage of bed	$\varepsilon = 0.4$

The gas and solid temperatures, $t_g(i+1,j)$ and $t_s(i,j+1)$, are calculated using equations (45) to (54), from point (i,j). Fig. 7 shows the gas and solid temperature profile in the 50^{th} section after ignition. Fig. 8 shows the solid temperature profile in the 50^{th} zone from the top of bed.

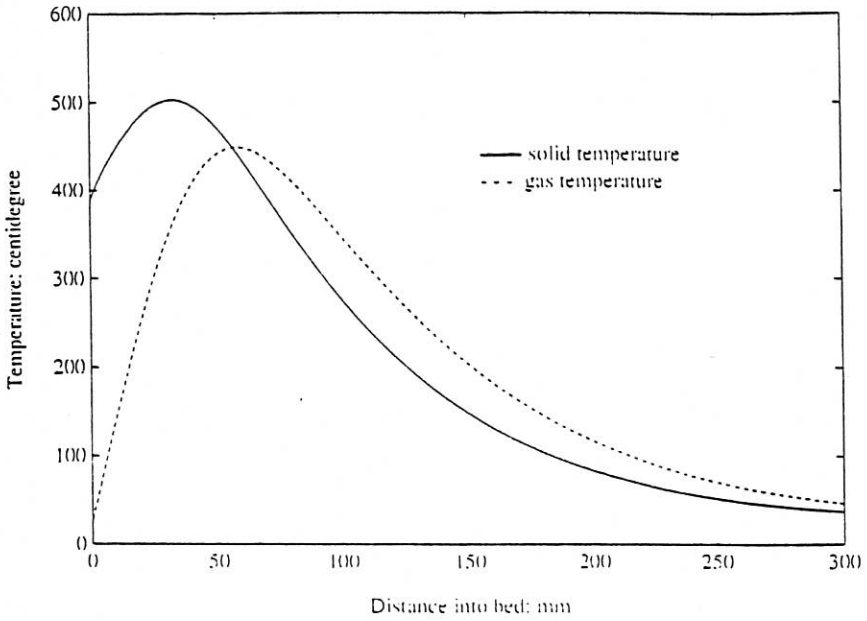

Fig. 7 Solid and Gas Temperature by Convective Heat Exchange

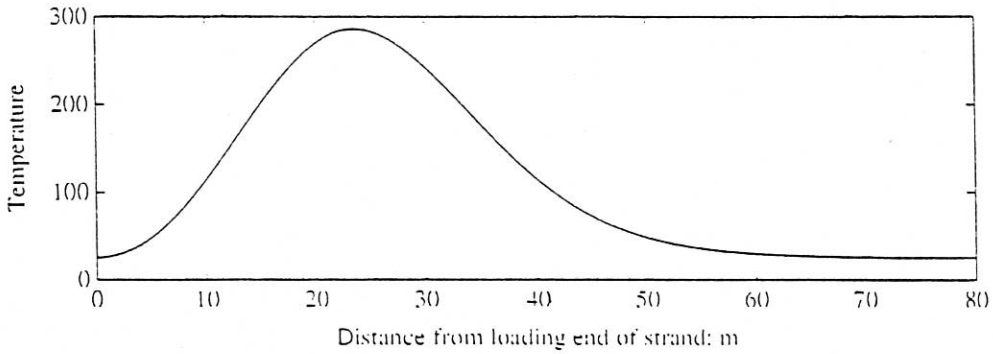

Fig. 8 Solid Temperature in a Zone by Convective Heat Exchange

Static Simulation of Sinter Plant

When the sintering process is proceeding if the operating conditions stay constant the variables included in the sintering process are also constant and the process is in its steady state. The modelling of the various phases of the sintering process have already been discussed. Implementation of the model is based on the method used for the simulation of convective heat exchange but various phases of the sintering process are included, where the element on the i^{th} zone and j^{th} section may lie in any one of the following regions:

1. cooling
2. cooling and solidification

3. fusion (melting)
4. coke combustion and melting
5. heating and coke combustion
6. convective heating
7. limestone decomposition
8. drying (moisture evaporating)
9. heating and condensing

depending on the solid temperature of the element. The results of simulation indicate the stable state of the sintering process.

The temperature of gas in all regions and on each point in the depth-time plane is given by:

$$t_g(i+i,j) = t_g(i,j) + \frac{\Delta x a h_p(i,j)}{\varepsilon u(i,j) P_g(i,j) C_g(i,j)} [t_s(i,j) - t_g(i,j)] \tag{55}$$

Some variables of gas phase are given a discrete form in Equ. (47)(48)(51)(52)(54), others are given here.

Convective heat transfer coefficient between gas and solid:

$$h_p(i,j) = \frac{\lambda(i,j)}{\varepsilon d_p(i,j)} [2.0 + 0.71 P_r^{1/3}(i,j) R_e^{1/2}(i,j)] \tag{56}$$

Reynolds number:

$$R_e = \varepsilon P_g(i,j) d_p(i,j) u(i,j) / \mu(i,j) \tag{57}$$

the gas velocity $u(i,j)$ is calculated by discrete Ergun equation:

$$-\frac{p(i+1,j) - p(i,j)}{\Delta x} = 150 \frac{(1-\varepsilon)^2}{\varepsilon^3 d_p^2(i,j)} \mu(i,j) u(i,j) + 1.75 \frac{1-\varepsilon}{\varepsilon^2 d_p(i,j)} P_g(i,j) u^2(i,j) \tag{58}$$

$$\frac{p(i+1,j) - p(i,j)}{\Delta x} = -\frac{\Delta P}{A h(j)} \tag{59}$$

Oxygen content in gas mixture:

$$C_{O_2}(i+1,j) = C_{O_2}(i,j) - \frac{\Delta x}{\varepsilon u(i,j)} R_c(i,j) \tag{60}$$

Carbon dioxide content in gas mixture:

$$C_{CO_2}(i+1,j) = C_{CO_2}(i,j) + \frac{\Delta x}{\varepsilon u(i,j)} [R_c(i,j) + R_l(i,j)] \tag{61}$$

Moisture content in gas mixture:

$$C_{H_2O}(i+1,j) = C_{H_2O}(i,j) + \frac{\Delta x}{\varepsilon u(i,j)} R_H(i,j) \tag{62}$$

The temperature of solid in all regions and on each point in the depth-time plane is given by the discrete form of Equ. (16) as follows:

$$t_s(i,j+1) = t_s(i,j) + \frac{\Delta t a(i,j) h_p(i,j)}{P_s(i,j) C_s(i,j)} [t_g(i,j) - t_s(i,j)] + \frac{\Delta t [H_c R_c(i,j) + Q_a(i,j)]}{P_s(i,j) C_s(i,j)} \tag{63}$$

In practice the solid temperature is worked out by omitting the term $Q_a(i,j)$ in equation (63), then this temperature is modified by considering the effect of additional heat produced in the different sub-process phase.

Other variables of the solid phase are given the discrete expression in the following.

Apparent density of bed:

$$P_s(i,j+1) = P_s(i,j) - \Delta t M_c R_c(i,j) - \Delta t M_{H_2O} R_H(i,j) - \Delta t M_{CO_2} R_l(i,j) \tag{64}$$

Specific surface area of solid particles per unit of bed:

$$a(i,j) = \frac{6(1-\varepsilon)}{d_p(i,j)} \tag{65}$$

Overall combustion rate of coke:

$$R_c(i,j) = 4\pi r_c^2(i,j) N_c K(i,j) C_{O_2}(i,j) \tag{66}$$

The number of coke particles in the per unit volume solid is obtained from the initial conditions. The radius of coke particles is given by:

$$r_c(i,j+1) = r_c(i,j) - \Delta t\, 12\times10^{-3} K(i,j) C_{O_2}(i,j) / P_c \tag{67}$$

$$K(i,j) = \frac{K_c(i,j) K_m(i,j)}{K_c(i,j) + K_m(i,j)} \tag{68}$$

The coefficient of mass transfer:

$$K_m(i,j) = \frac{D_{ON}(i,j)}{\varepsilon d_p(i,j)} [2.0 + 0.75 S_c^{1/3}(i,j) R_e^{1/2}(i,j)] \tag{69}$$

The chemical combustion rate constant:

$$K_c(i,j) = 6.52\times10^5 e^{-\frac{18500}{Rt_s(i,j)}} \sqrt{t_s(i,j)} \tag{70}$$

The diffusion coefficient of oxygen through nitrogen:

$$D_{ON}(i,j) = 1.8\times10^{-5} [\frac{t_g(i,j)}{273}]^{3/2} \tag{71}$$

Schmidt number:

$$S_c(i,j) = \frac{\mu(i,j)}{P_g(i,j) D_{ON}(i,j)} \tag{72}$$

The combustion of coke occurs when the radius of coke particles is greater than zero.

The additional heat supplied to (or drawn from) the bed depends upon the process phase on which the calculated element of the bed lies. For the different process phase the additional heat is calculated individually by the following equations.

For the moisture evaporating from solid, additional heat drawn from the bed:

$$Q_a(i,j) = \begin{cases} \dfrac{P_s(i,j)C_s(i,j)[100 - t_s(i,j+1)]}{\Delta t} & \text{if } \rho_{H_2O}(i,j) > 0,\ t_s \geq 100^o C \\ 0 & \text{if } \rho_{H_2O}(i,j) = 0 \end{cases} \tag{73}$$

exchange rate of moisture from solid phase to gas phase:

$$R_H(i,j) = - Q_a(i,j) / H_w \tag{74}$$

For the condensing of moisture from gas phase to solid phase, the additional heat supplied to bed:

$$Q_a(i,j) = \begin{cases} \dfrac{\varepsilon u(i,j)P_g(i,j)[60 - t_g(i+1,j)]}{\Delta x} & \text{if } C_{H_2O} > 0,\ t_g \leq 60^o C \\ 0 & \text{if } C_{H_2O}(i,j) = 0 \end{cases} \tag{75}$$

exchange rate of moisture from gas phase to solid phase:

$$R_H(i,j) = - Q_a(i,j) / H_w \tag{76}$$

where H_w is the latent heat of moisture.

For the limestone decomposition, the additional heat drawn from bed:

$$Q_a(i,j) = \begin{cases} F_l \dfrac{P_s(i,j)C_s(i,j)[t_{sl} - t_s(i,j+1)]}{\Delta t} & \text{if } \rho_l(i,j) > 0,\ t_s(i,j+1) \geq 600^o C \\ 0 & \text{if } \rho_l(i,j) = 0 \end{cases} \tag{77}$$

limestone decomposition rate:

$$R_l(i,j) = -\,Q_a(i,j) \,/\, H_l \tag{78}$$

where F_l stands for the heat fraction of limestone decomposition (less than 1). H_l stands for the reduction heat of limestone decomposition. t_{sl} is a calculated constant, $t_{sl} = 600^o C$, if $t_s(i,j) < 600^o C$ or $t_{sl} = t_s(i,j)$, if $t_s(i,j) \geq 600^o C$.

For the melting of solid mixture, additional heat drawn from bed:

$$Q_a(i,j) = \begin{cases} F_m \dfrac{P_s(i,j)C_s(i,j)[T - t_s'(i,j+1)]}{\Delta t} & \text{if } t_s(i,j+1) \geq T \\ 0 & \text{if } t_s(i,j+1) < T \end{cases} \tag{79}$$

the melting heat stored in the form of latent heat:

$$Q_f(i,j+1) = Q_f(i,j) - \Delta t Q_a(i,j) \tag{80}$$

the solid temperature is modified by the following equation:

$$t_s(i,j+1) = t_s'(i,j+1) - F\,[t_s'(i,j+1) - T\,] \tag{81}$$

where $t_s'(i,j+1)$ is the solid temperature obtained without considering the melting.

For the solidification of the solid mixture, additional heat supplied to bed:

$$Q_a(i,j) = \begin{cases} F_l \dfrac{\varepsilon P_g(i,j)C_g(i,j)u(i,j)[t_g(i+1,j) - t_g(i,j)]}{\Delta x} & \text{if } Q_f(i,j) > 0 \\ 0 & \text{if } Q_f(i,j) \leq 0 \end{cases} \tag{82}$$

melting heat stored in the form of latent heat:

$$Q_f(i,j+1) = Q_f(i,j) - \Delta t Q_a(i,j) \tag{83}$$

solid temperature is modified by the following equation:

$$t_s(i,j+1) = t_s'(i,j+1) + \frac{\Delta t Q_a(i,j)}{P_s(i,j)C_s(i,j)} \tag{84}$$

melting time is given by:

$$\tau(i,j+1) = \tau(i,j) + \Delta t \qquad \text{if } t_s(i,j+1) \geq T \tag{85}$$

mean pellet diameter growing is given by:

$$d_p(i,j+1) = d_p(i,j) + \Delta t B \tag{86}$$

$$B = \frac{d_{p_F} - d_{p_I}}{\Gamma} \tag{87}$$

where

d_{p_F} is the final mean pellet diameter.

d_{p_I} is the initial mean pellet diameter.

Γ is the total melting time.

The melting fraction index is calculated by:

$$f(i) = 1 - [\ 1 - 2V\Gamma(i) / d\ ]^3 \tag{88}$$

suppose that the particle diameter d_j and the dry porosity ε_j are uniform.

here $\Gamma(i)$ is the total melting time of the solid in the i^{th} zone.

Considering that each zone holds the same quantity of solid material in a section of bed, therefore the average melting fraction index in a section of bed is given by:

$$f = \frac{1}{n}\sum_{i=1}^{i=n} f(i) \tag{89}$$

Given a set of initial and boundary conditions as follows:

initial solid temperature	$t_s(i,0) = 25^o C \qquad i=0,\ldots\ldots,n$
gas temperature for ignition	$t_g(0,j) = 1180^o C \qquad j=0,\ldots\ldots,L_h$
gas temperature after ignition	$t_g(0,j) = 25^o C \qquad j=L_h+1,\ldots\ldots,m$
suction of the fan	$\Delta P = 600000\ Kg\ m\ /\ s^2$
strand speed	$v = 4.2\ m\ /\ \min$
oxygen content in gas	$C_{O_2}(0,j) = 8.92\ mol\ /\ m^3$
carbon dioxide content in gas	$C_{CO_2}(0,j) = 0.0\ mol\ /\ m^3$
nitrogen content in gas	$C_{N_2} = 35.68\ mil\ /\ m^3$
moisture in gas	$C_{H_2O}(0,j) = 0.0\ mol\ /\ m^3$
limestone addition in mixture	$X_3 = 6.0\ \%$
coke addition in mixture	$X_4 = 5.5\ \%$
water addition in mixture	$X_w = 5.0\ \%$
mean pellet diameter	$d_p(i,0) = 3\ mm$

and given the following constants:

length of strand	$L = 80\ m$
width of strand	$W = 4\ m$
height of bed	$h = 300\ mm$
ignition period	$L_h = 100$
voidage of bed	$\varepsilon = 0.4$

The solid and gas temperature are calculated simultaneously. Fig. 9 shows the gas and solid temperature profile in the 300^{th} section after ignition, Fig. 10 shows the solid temperature profile at the bottom of bed, Fig. 11 shows the profile of oxygen and carbon dioxide concentration in exhausted gas from the strand and Fig. 12 shows the velocity of exhausted gas from the strand.

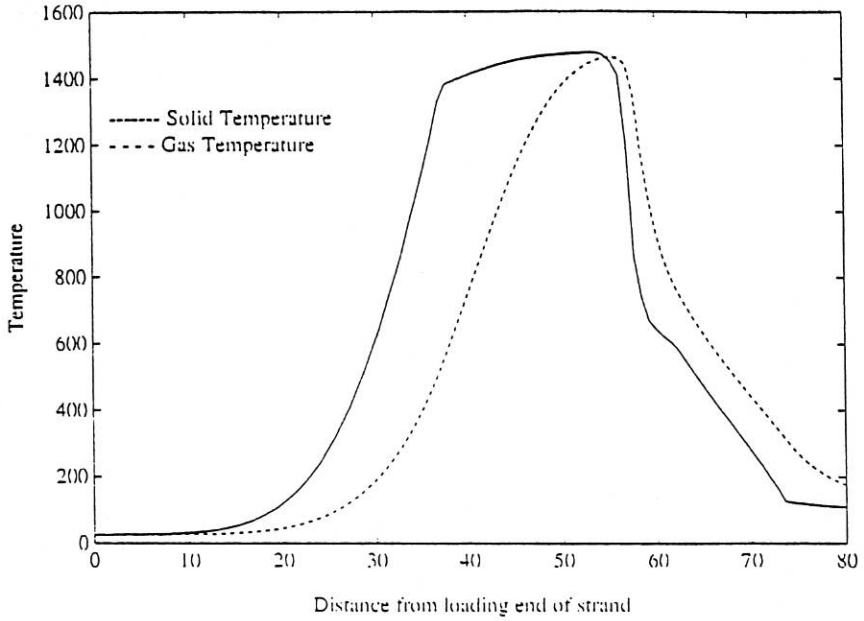

Fig. 9 Solid and Gas Temperature Profile in a Section

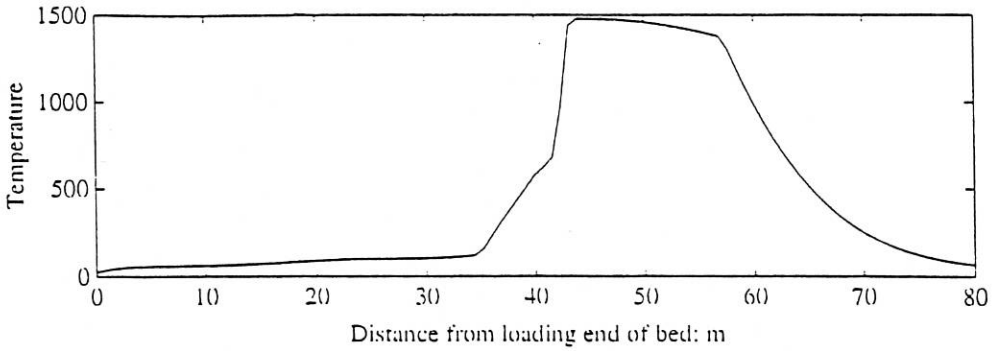

Fig. 10 Solid Temperature Profile at Bottom of Bed

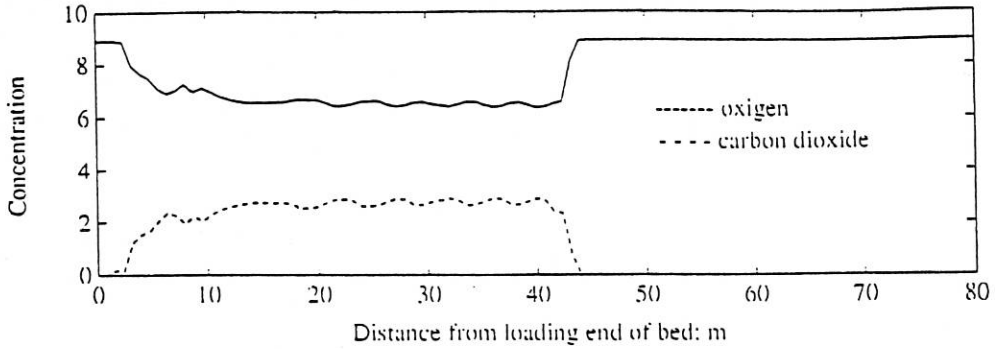

Fig. 11 Oxygen and Carbon Dioxide Content in Exhaust Gas

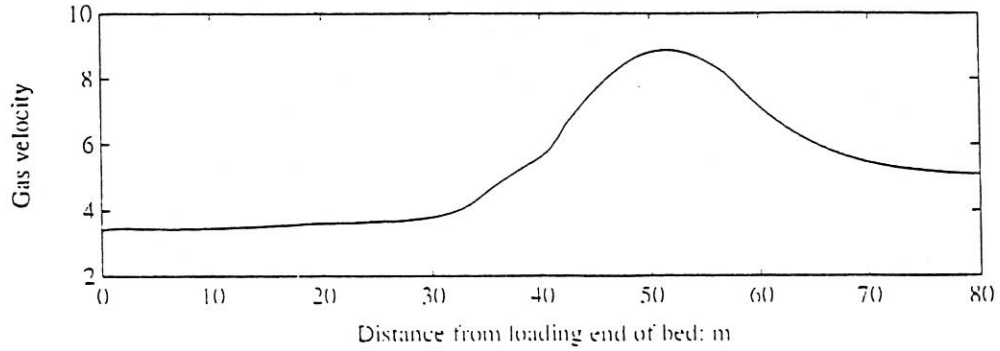

Fig. 12 Velocity of Exhaust Gas Under Strand

INVESTIGATION OF SINTERING PROCESS BY SIMULATION

Any change of an operating condition or input variable affects the process state variables and finally affects the production quality which is probably the most important output variable and the most difficult one to measure continuously. It is more desirable to have a consistent quality and a steady process performance in a long operating period rather than a high average quality. The aim of adjusting the operating condition is to obtain the required quality of sinter production. This investigation is concentrated on the study to the change of the measurable process outputs and the important performance of the process while the operating conditions or input variables are changed. Obviously the sinter plant is a multi-input, multi-output system. An output variable is connected to several input variables. Fig.13 shows the relationship between variables. A sumary is given in Table.1 to show the effect of changing operating conditions and input variables on the process. Based on the conditions selected for running this simulation algorithm the qualitative analysis is presented.

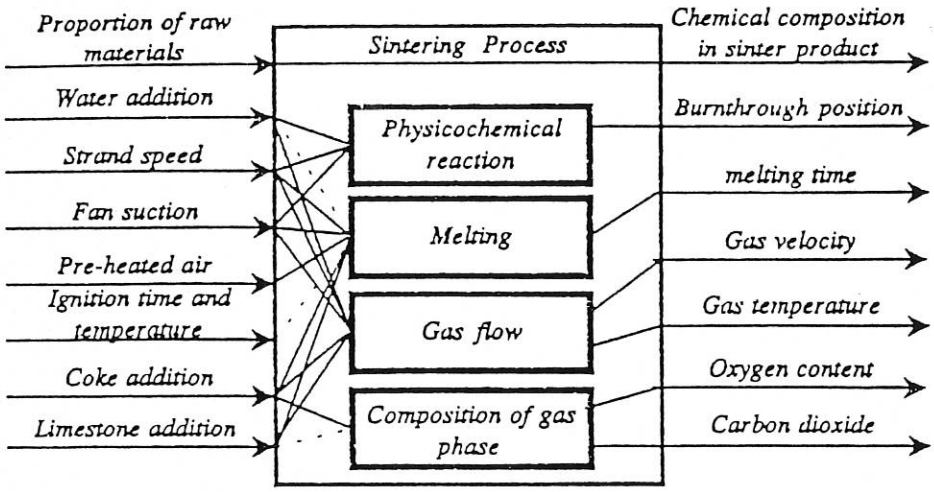

Fig. 13 Relation Between Variables

Items	Adjustment Range **	Burnthrough Position	Fusion Zone	Melting Time	Temperature and Velocity of Gas	Carbon Dioxide and Oxygen of Gas
Coke-addition (%)	*3.5 - 7.5	——	GREAT	GREAT	YES	YES
Water-addition (%)	5.0 - *13.0	GREAT	MEDIUM	SLIGHT	YES	——
Limestone-addition (%)	3.0 - *15.0	——	MEDIUM	MEDIUM	YES	SLIGHT
Strand Speed (m / min)	2.2 - *6.2	GREAT	——	GREAT	YES	——
Fan Suction (Kg m / squ.s)	*490000 - - 2450000	GREAT	SLIGHT	SLIGHT	YES	——
Ignition Time (s)	*61.6 - 159.6	——	——	SLIGHT	——	——
Ignition Temperature (C)	*760 - 1180	——	——	——	——	——
Pre-heated Air	Used or Not	——	MEDIUM	IMPROVED	——	——

* Crtical value for that variable ** Selected to ensure successful ignition

Table 1 Effect on The Process of Changing Operating Conditions and Input Variables

Ignition

It is well recognized that good ignition is essential not only for the production of strong sinter in the upper layers but also that the heat front is properly established. If the ignition is successful the heat front is established and a required fusion zone would be formed.

The variation in coke addition plays an important role in ignition, the reason is straightforward; too little coke cannot provide enough heat for the formation of fusion zone after the ignition time. The least addition of coke for successful sintering is limited to be 3.5 %. Fig.14 and Fig.15 show this limitation. Less coke addition than this value results in failure of ignition.

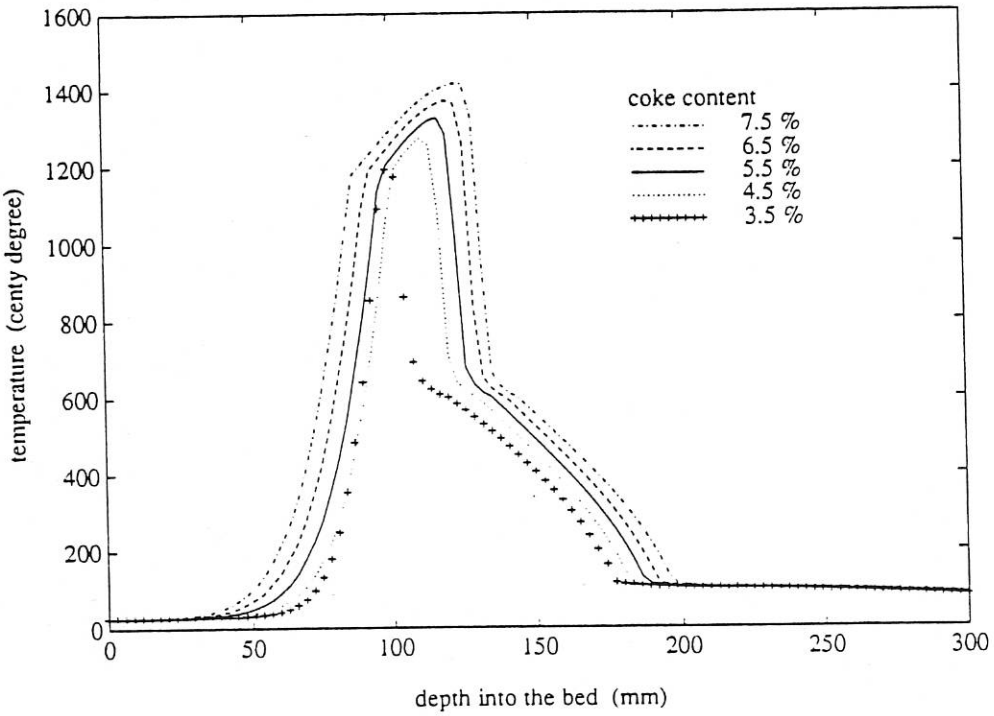

Fig. 14 Effect of Changing Coke-addition on Solid Temperature in a Section

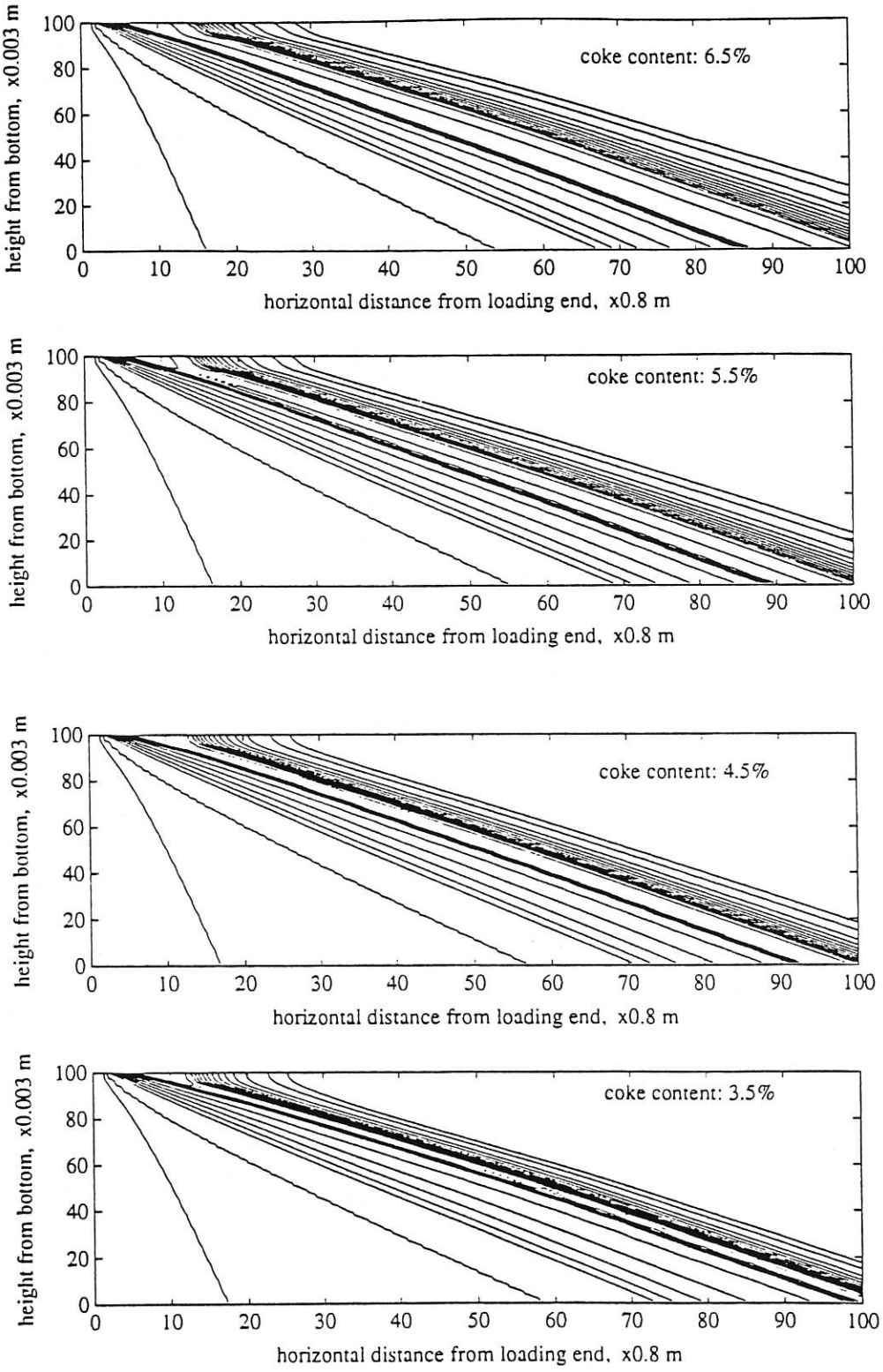

Fig. 15 Effect of Changing Coke-addition on Sintering Process in Bed

A change in water-addition affects the ignition in two ways; an increase in water-addition increases the mean pellet diameter of the mixture. The larger mean pellet diameter results in a lower convective heat transfer coefficient between the particles and gas, also a lower specific solid area per unit volume of bed. Therefore the solid mixture will acquire less heat from hot air in the ignition region, and will not readily giving up heat to the cold air drawn in after ignition. On the other hand, the increase of water content in the mixture needs more heat to raise the solid temperature. Finally the cold air is allowed to reach the combustion zone and the sintering process ceases. The water-addition should be less than 11 % according to the result of the simulation, shown in Fig.16 and Fig.17.

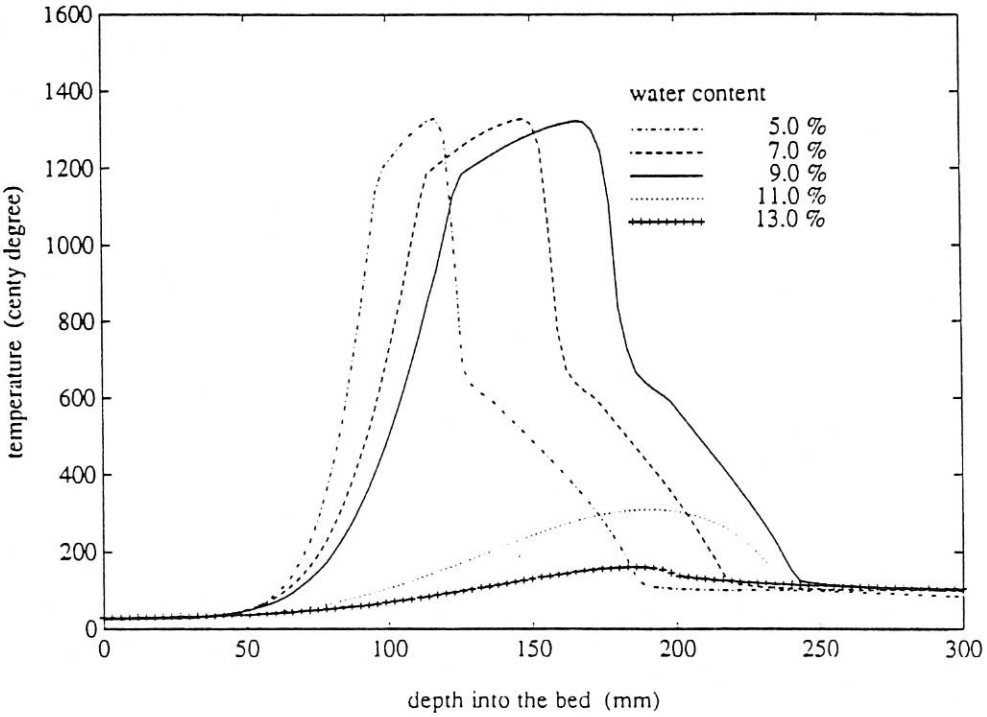

Fig. 16 Effect of Changing Water-addition on Solid Temperature in a Section

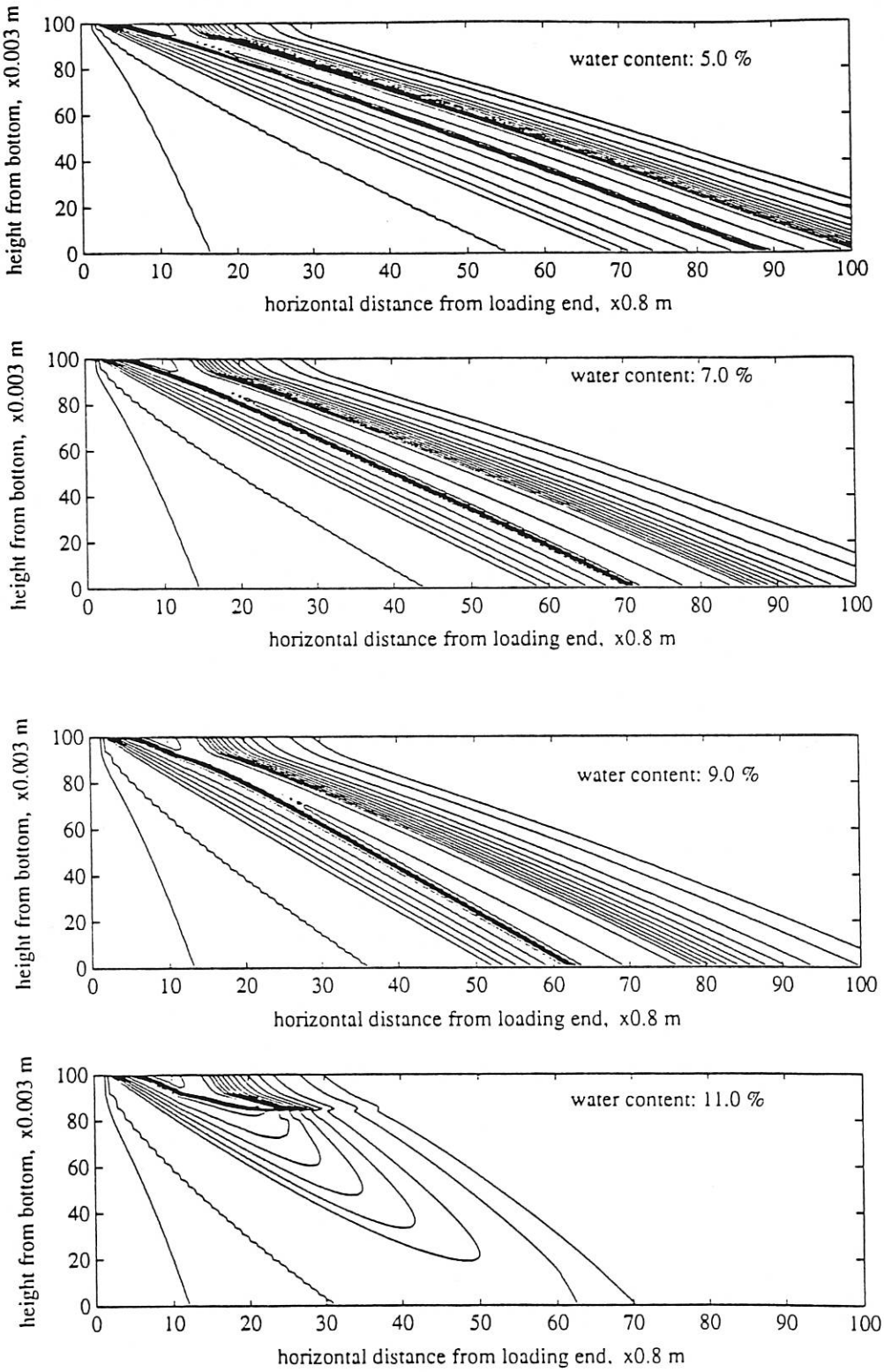

Fig. 17 Effect of Changing Water-addition on Sintering Process in Bed

A change of limestone addition affects the ignition only when the limestone content in the mixture is too much. This is because the more limestone content needs more heat for decomposition and less heat is provided to heat the solid mixture. The results of simulation, shown in Fig.18 and Fig.19, indicate that the ignition will fail if the limestone addition exceeds a critical figure of 15 %.

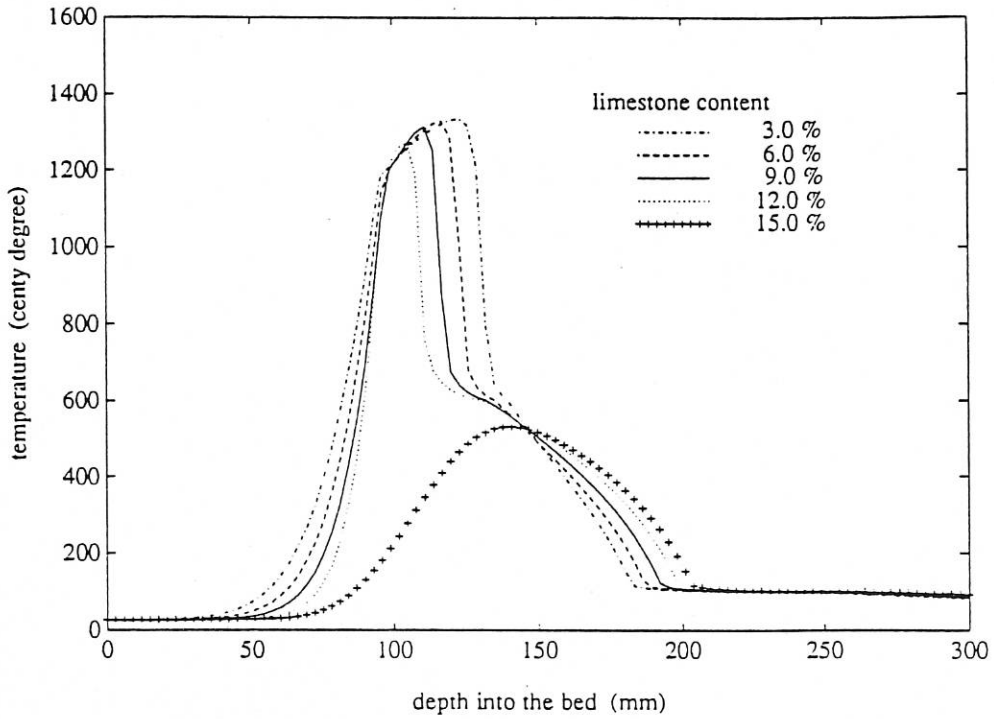

Fig. 18 Effect of Changing Limestone-addition on Solid Temperature in a Section

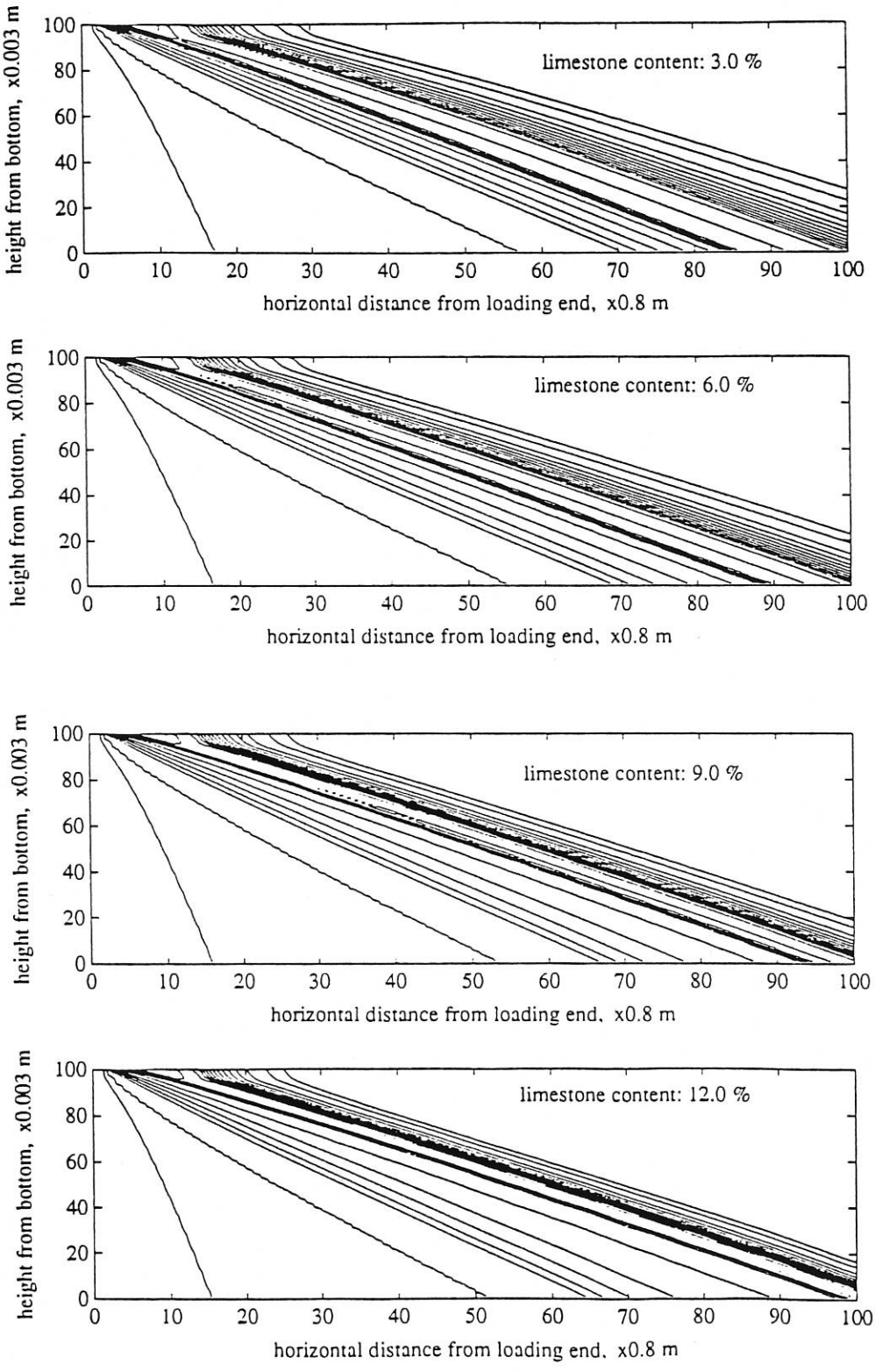

Fig. 19 Effect of Changing Limestone-addition on Sinering Process in Bed

With regard to ignition, a change in strand speed is equivalent to a change in the ignition time. The shorter the mixture is in the ignition region, the less the mixture obtains the heat from the hot air. The strand speed cannot be faster than 6.2 *m/min* and ignition time cannot be less than 75.8 *s* in this simulation according to the results shown in Fig.20, Fig.21, Fig.22 and Fig.23.

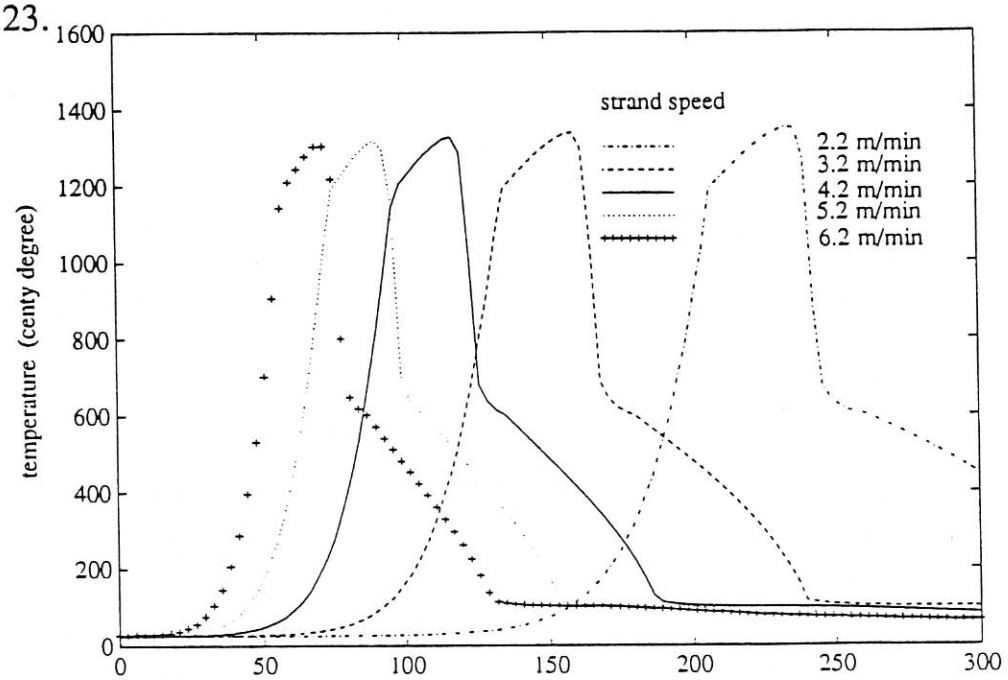

Fig. 20 Effect of Changing Strand Speed on Solid Temperature in a Section

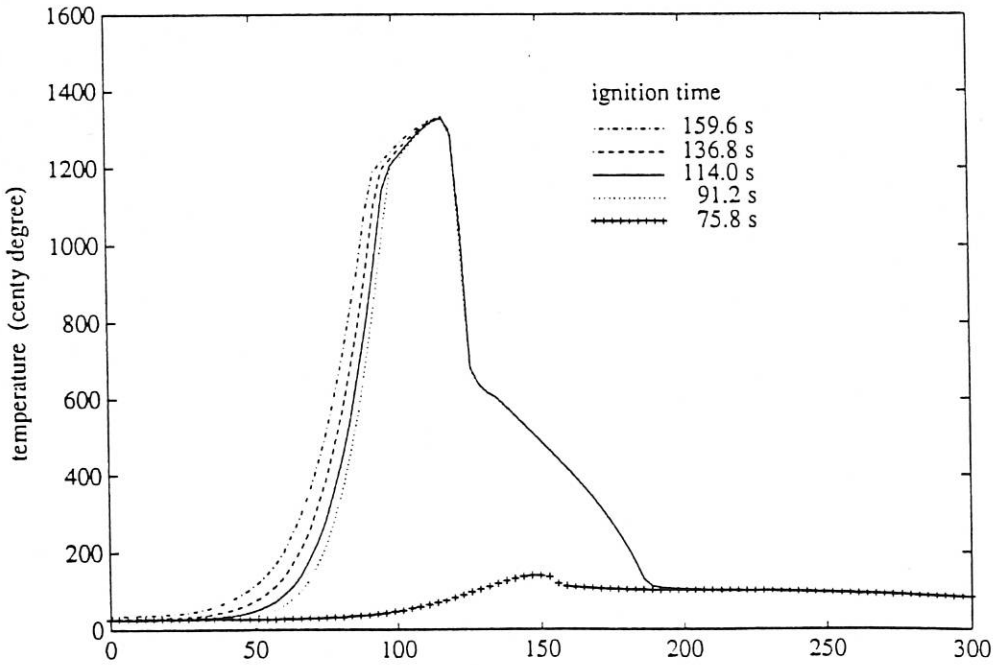

Fig. 21 Effect of Changing Ignition Time on Solid Temperature in a Section

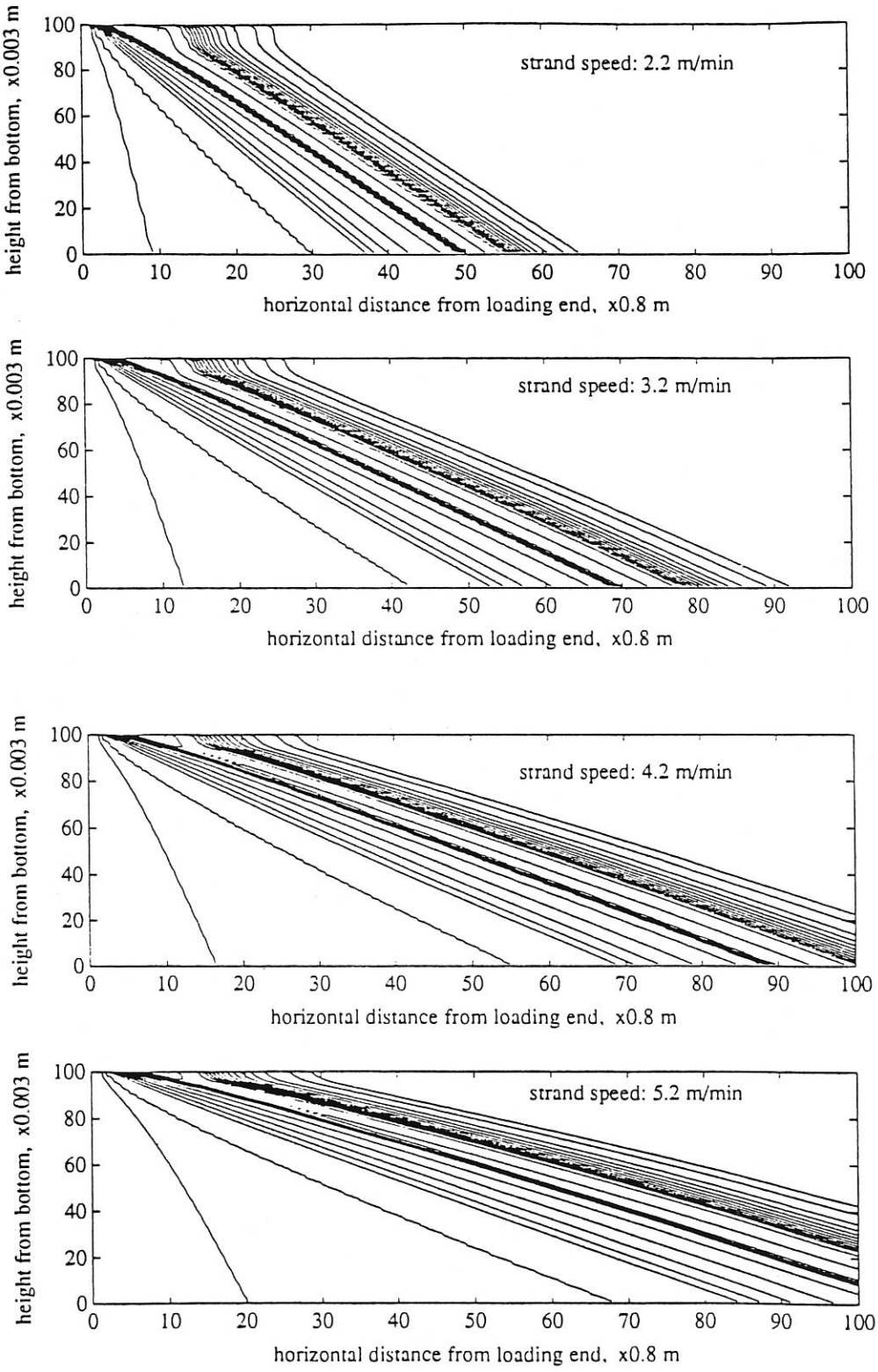

Fig. 22 Effect of Changing Strand Speed on Sintering Process in Bed

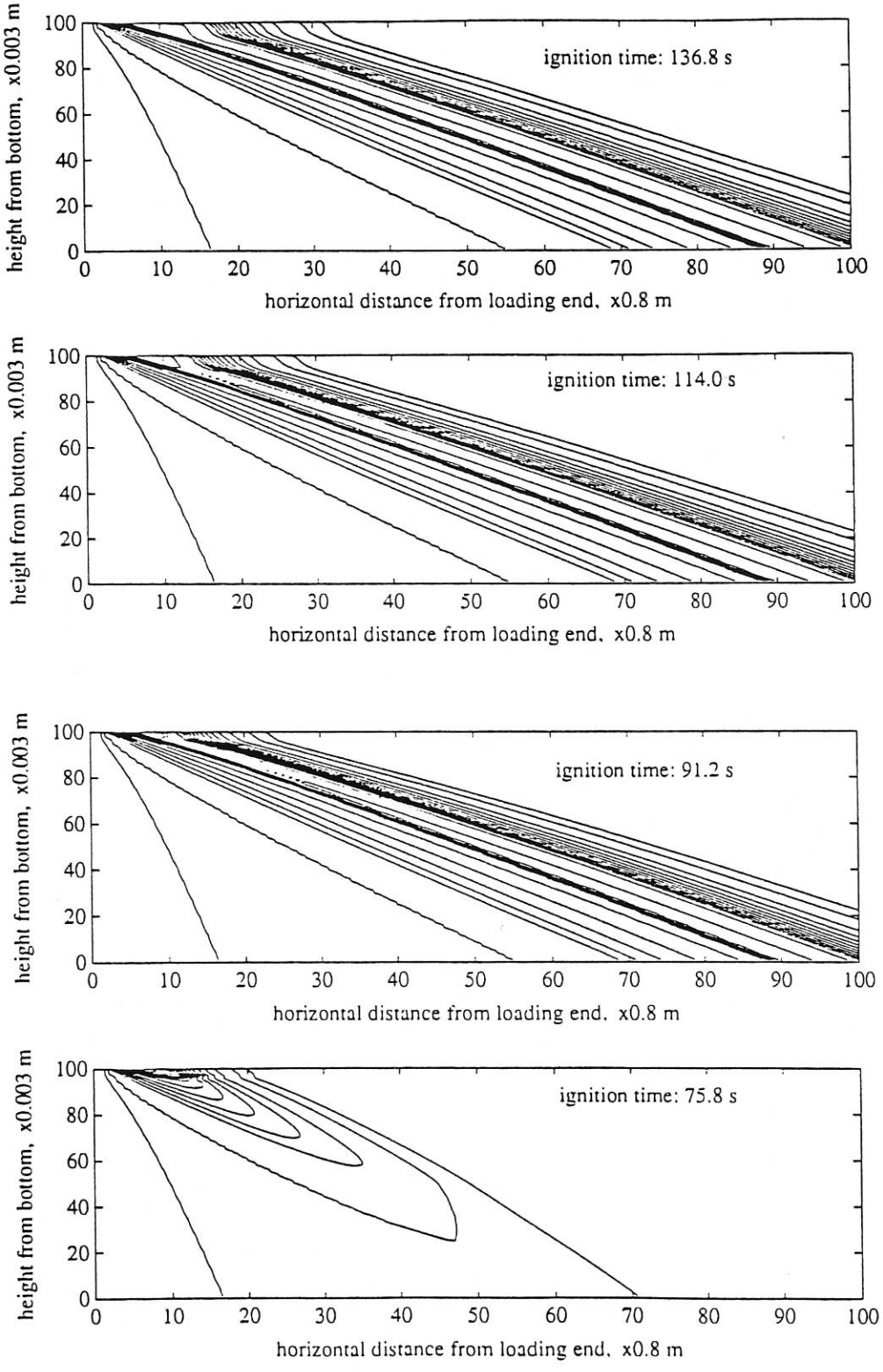

Fig. 23 Effect of Changing Ignition Time on Sintering Process in Bed

The ignition temperature does not normally affect ignition but the ignition temperature must not be lower than a critical value of about $780^{o}C$. This value is just higher than the temperature at which coke combustion can take place. This result is shown in Fig.24 and Fig.25.

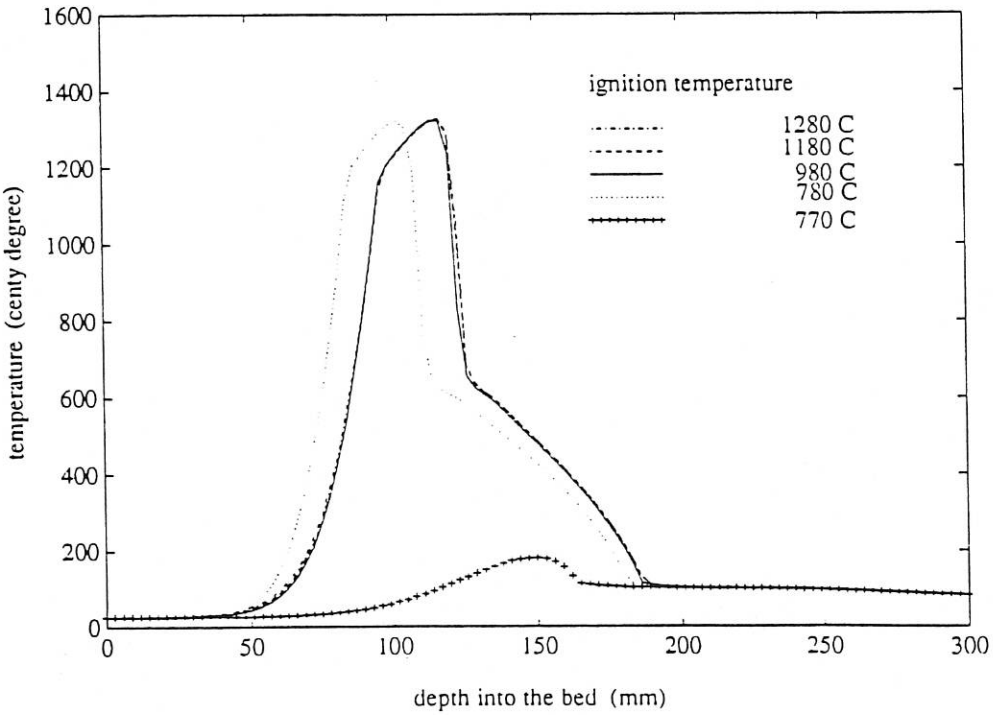

Fig. 24 Effect of Changing Ignition Temperature on Solid Temperature in a Section

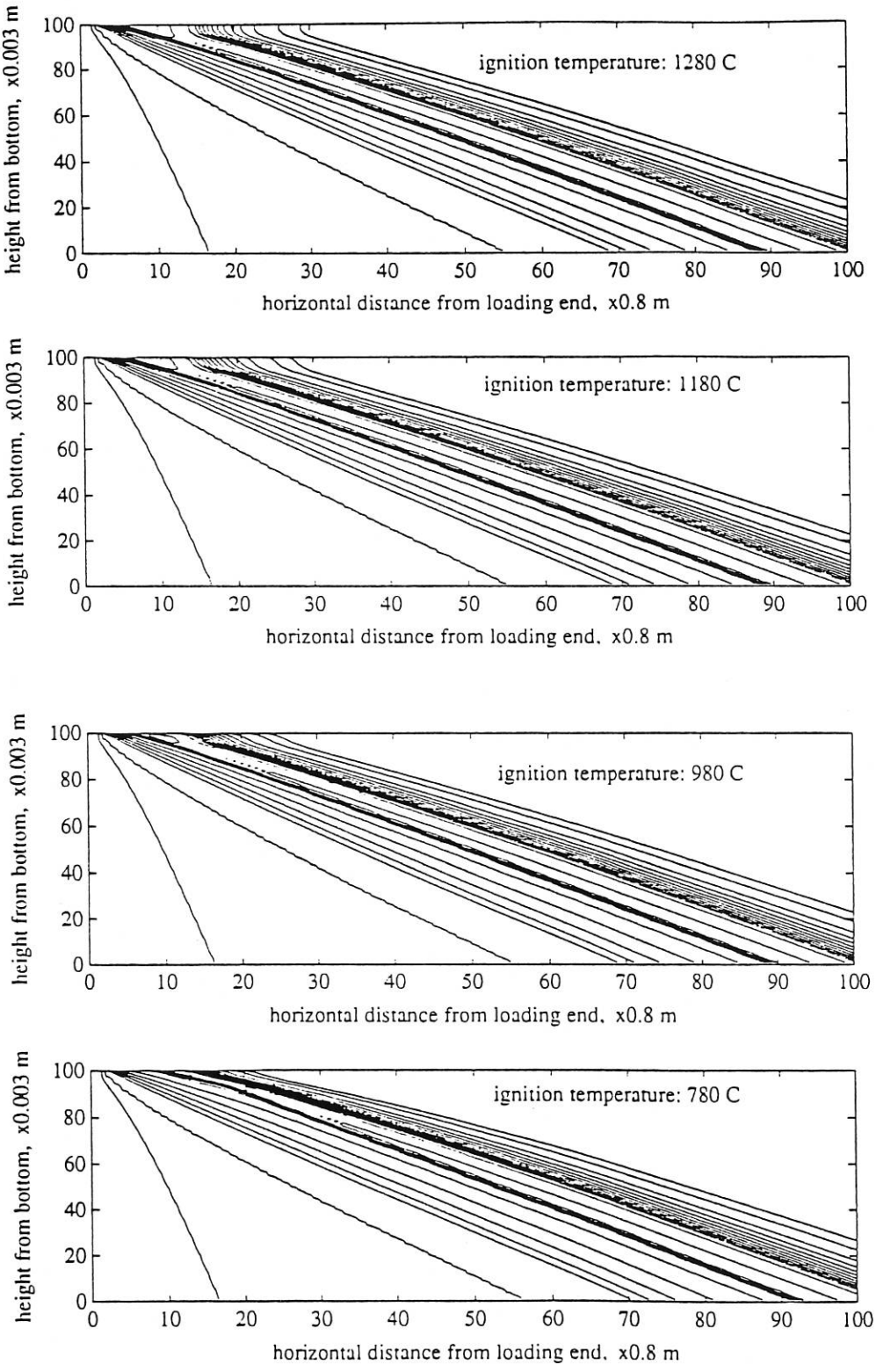

FIg. 25 Effect of Changing Ignition Temperature on Sintering Process in Bed

The Fig.26 and Fig.27 indicate that variation in fan suction has no effect on the ignition.

Unfortunately it could not be earlier detected whether the ignition is successful or not from the real sintering process, so it was necessary to carefully select the adjustment range of operating conditions and variables for the process to ensure that the ignition would not fail when adjusting operating conditions and variables in the simulation exercises.

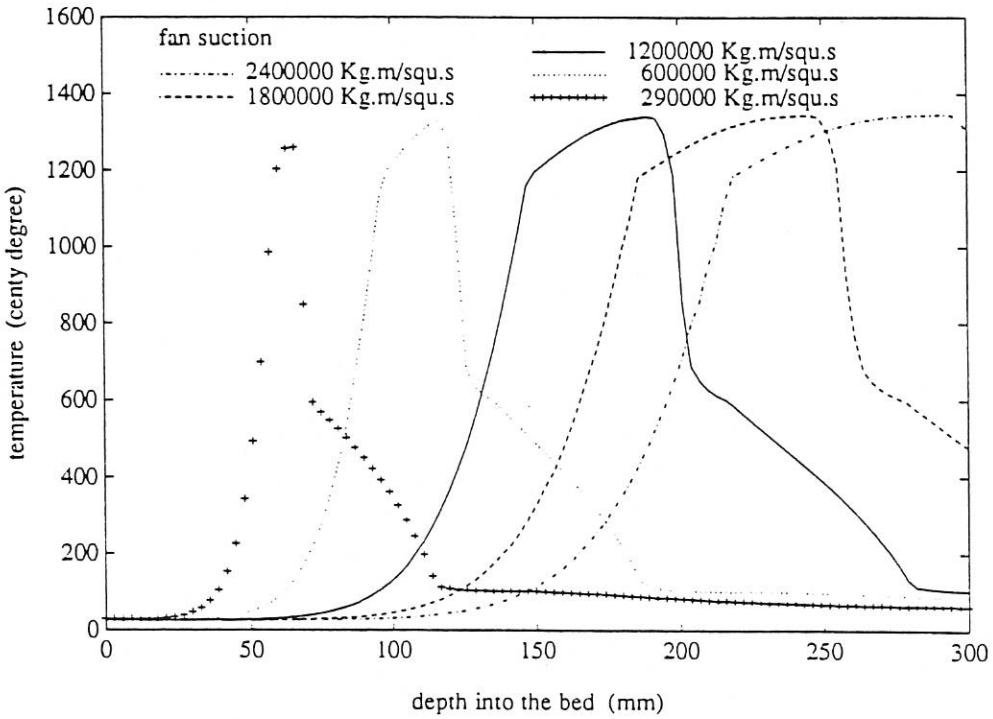

Fig. 26 Effect of Changing Fan Suction on Solid Temperature in a Section

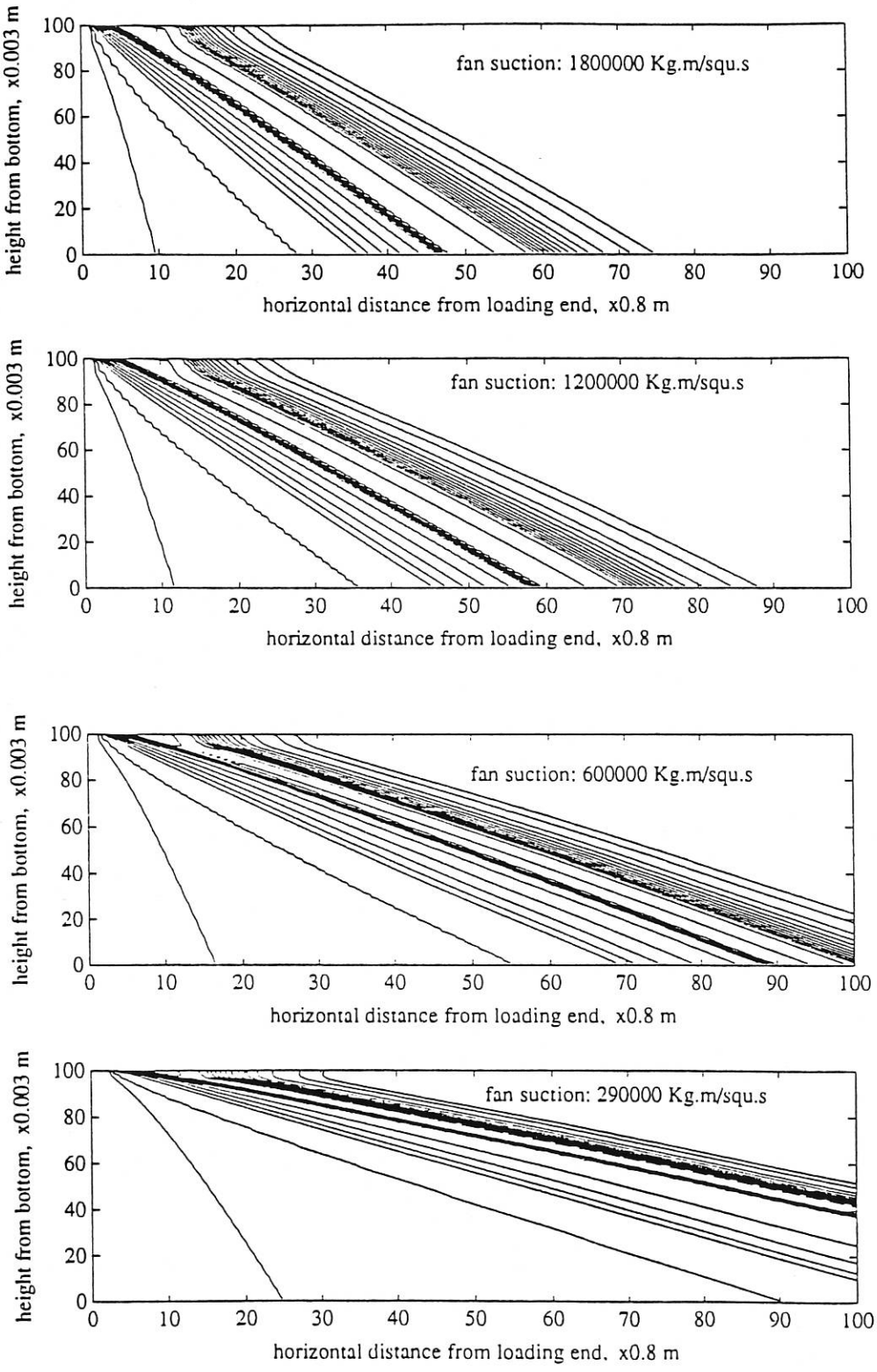

Fig. 27 Effect of Changing Fan Suction on Sintering Process in Bed

Burnthrough Position and Fusion Zone

Burnthrough position is defined as the position at which the combustion of coke in the mixture at the bottom of bed is completed and the solid temperature reduces to less than the melting temperature just before the sinter arrives at the end of the strand. Fusion zone is the high temperature region in which the mixture melts and the major chemicophysical reactions occur. The burnthrough position, fusion zone and how they are affected by changing in some of the operating condition and input variables to the process is discussed in here.

Basically the change of coke-addition does not affect burnthrough position. It only widens the fusion zone if the coke addition is increased because the more coke addition needs more time to complete its combustion. The Fig.15 and Fig.28 indicate this result.

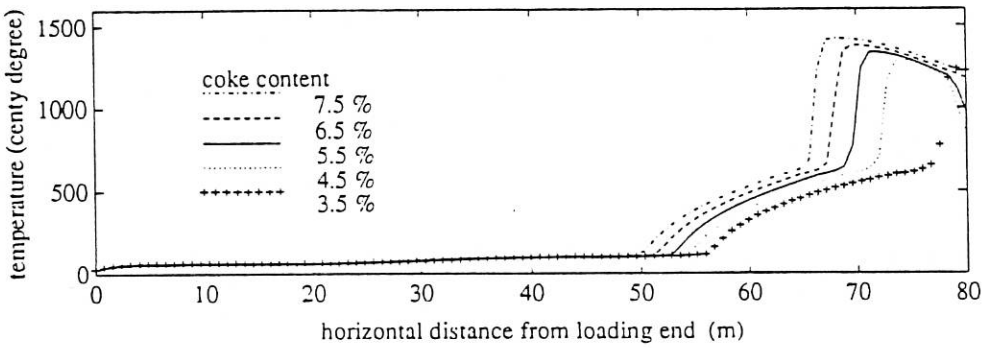

Fig. 28 Effect of Changing Coke-addition on Solid Temperature in a Zone

A change in water-addition greatly affects the burnthrough position and fusion zone as shown in Fig.17 and Fig.29. This is because the increase of water addition raises the gas flow rate (gas velocity) inside the bed by improving the permeability of bed, therefore, the speed of heat-wave propagation downward the bed is increased, which makes the sintering process complete earlier. This could benefit us to raise the production rate by increasing the water addition appropriately.

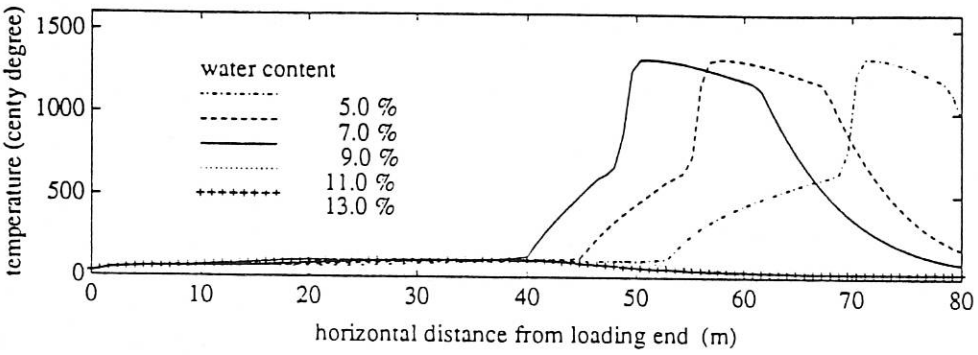

Fig. 29 Effect of Changing Water-addition on Solid Temperature in a Zone

It is indicated that a change in limestone addition does not affect the burnthrough position but fusion zone is changed in Fig.19 and Fig.30.

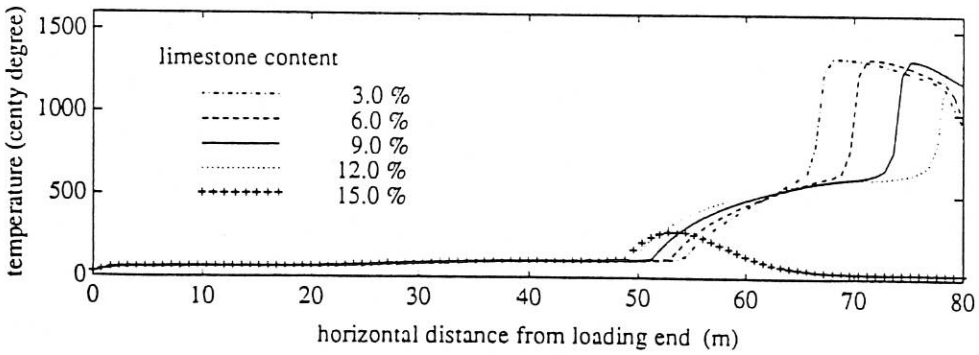

Fig. 30 Effect of Changing Limestone-addition on Solid Temperature in a Zone

A change of strand speed directly affects the burnthrough position, because the strand speed determines the time the solid mixture stays on the strand. It is the only effect which changing strand speed has on the

sintering process. Basically the strand speed has no effect on the fusion zone and the chemicophysical mechanism taking place during the sintering process provided successful ignition is guaranteed. This is shown in Fig.21 and Fig.31.

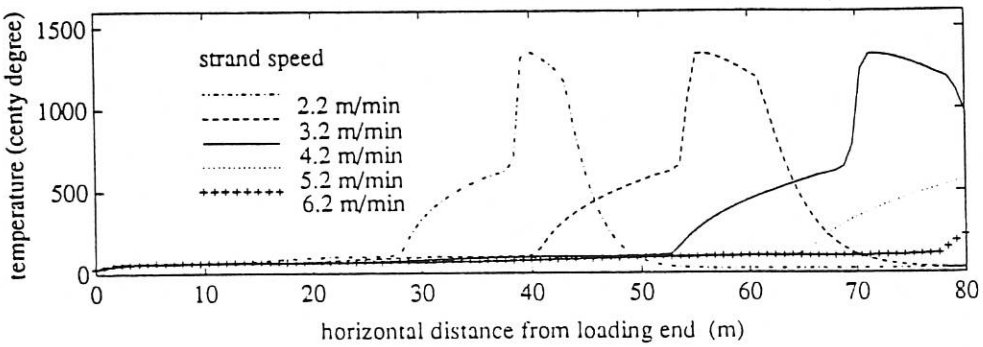

Fig. 31 Effect of Changing Strand Speed on Solid Temperature in a Zone

A change of ignition time and temperature also have no effect on the burnthrough position and fusion zone provided that the ignition is successful, shown in Fig.23, Fig.25, Fig.32 and Fig.33.

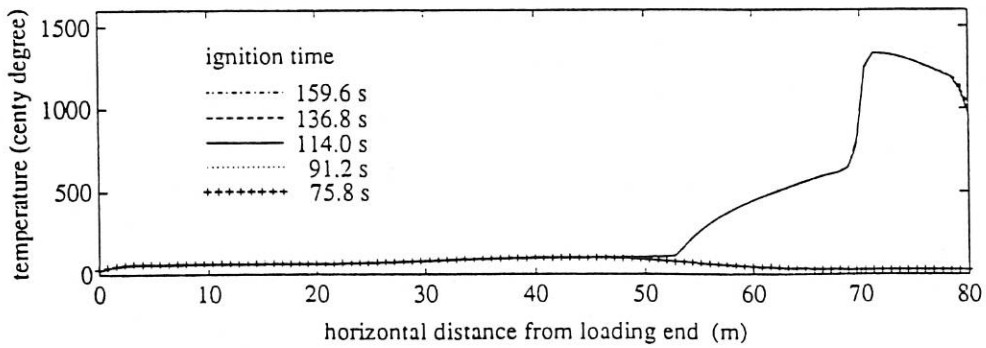

Fig. 32 Effect of Changing Ignition Time on Solid Temperature in a Zone

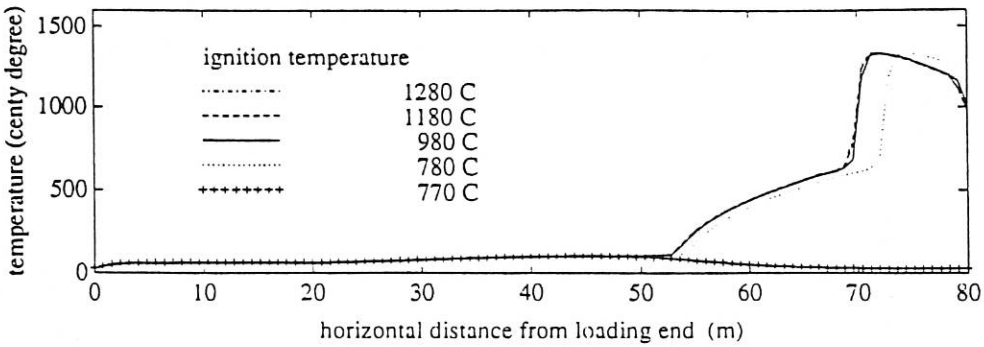

Fig. 33 Effect of Changing Ignition Temperature on Solid Temperature in a Zone

A change of fan suction directly affects the burnthrough position and slightly varies fusion zone, shown in Fig.27 and Fig.34. The chemicophysical reactions are completed faster by using a higher value of suction.

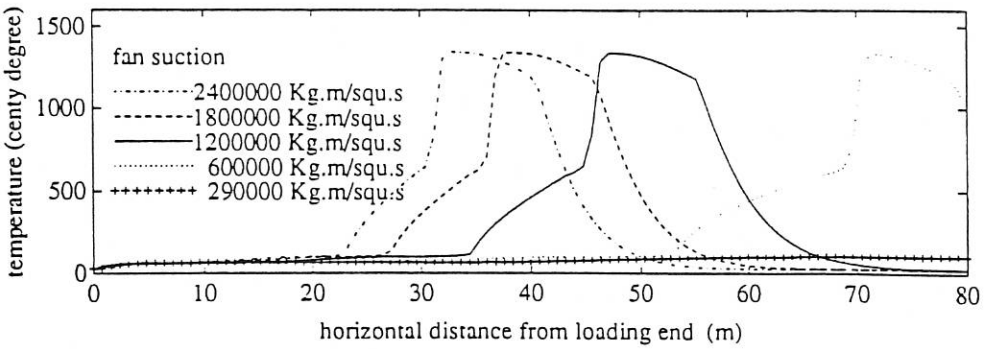

Fig. 34 Effect of Changing Fan Suction on Solid Temperature in a Zone

The burnthrough position and fusion zone can be detected by measuring the temperature or velocity of the exhausted gas underneath the strand at the selected positions.

Melting Time

Generally the melting time of solid mixture determines the quality of sinter product, including the size analysis which determines the permeability in the blast furnace, the hot strength so that the permeability is not degraded, the porosity to promote heat and mass exchange, the reducibility and mineral texture.

A change of coke-addition greatly affects the melting time. An increase in coke-addition results in a longer time taken by coke combustion, by which the solid mixture gets a longer period to stay in melting region. This is shown in Fig.35.

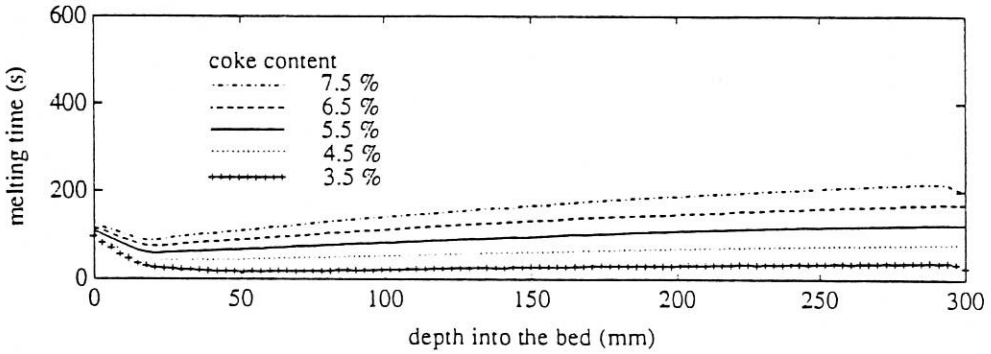

Fig. 35 Effect of Changing Coke-addition on Melting Time

As shown in Fig.36, a change of water-addition slightly affects the melting time (range of water-addition between 7.0 % – 11.0 %); this is because appropriately increased water addition improves the permeability of bed. Too great an addition could affect the ignition.

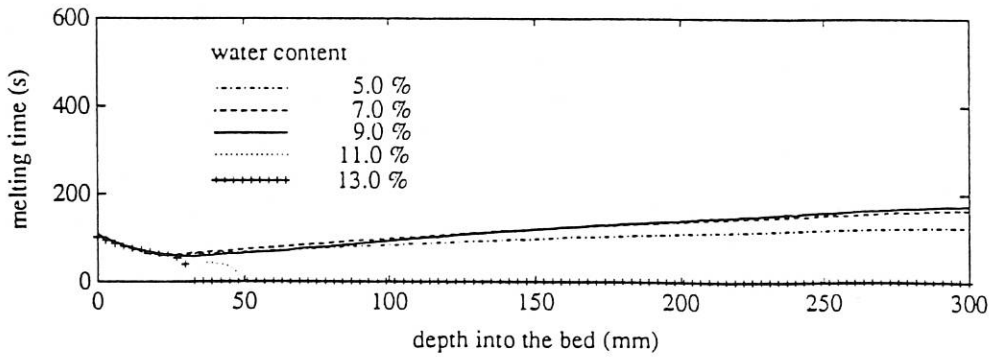

Fig. 36 Effect of Changing Water-addition on Melting Time

A change of limestone-addition obviously affects the melting time, shown in Fig.37. The limestone decomposition will take more heat from that to melt the solid mixture if more limestone is added.

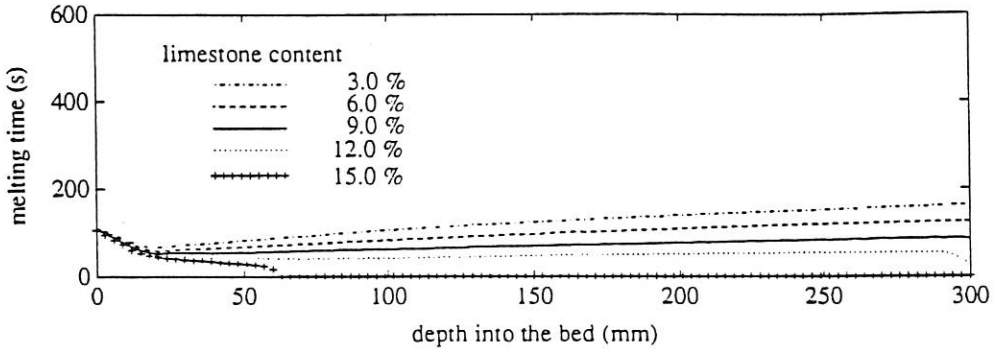

Fig. 37 Effect of Changing Limestone-addition on Melting Time

Change in strand speed affects the melting time in the different way, shown by Fig.38, depending upon whether the proper burnthrough position is obtained or not. If the strand is moving too fast the solid mixture will not be sinterred in the lower layer.

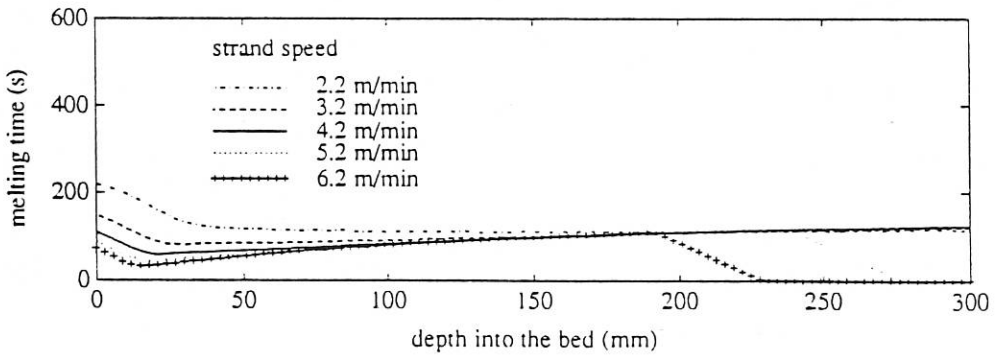

Fig. 38 Effect of Changing Strand Speed on Melting Time

Change of ignition time or temperature would not affect the melting time in the lower laid mixture if successful ignition is ensured. But the melting time of mixture in the upper layer is altered along with the change of ignition time or temperature. The Fig.39 and Fig.40 show this result.

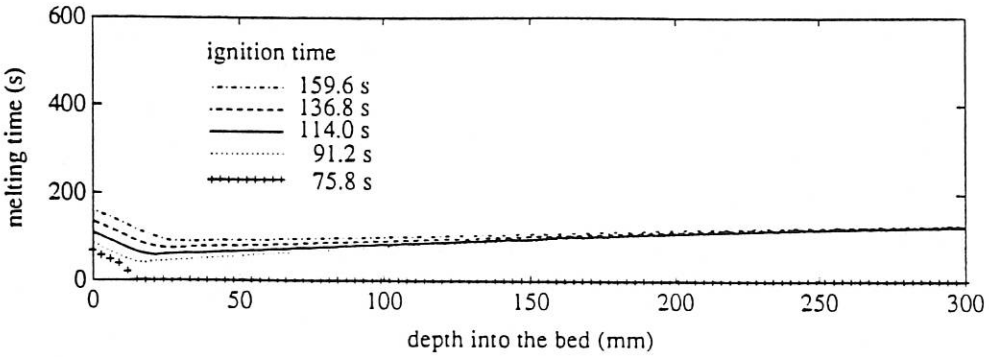

Fig. 39 Effect of Changing Ignition Time on Melting Time

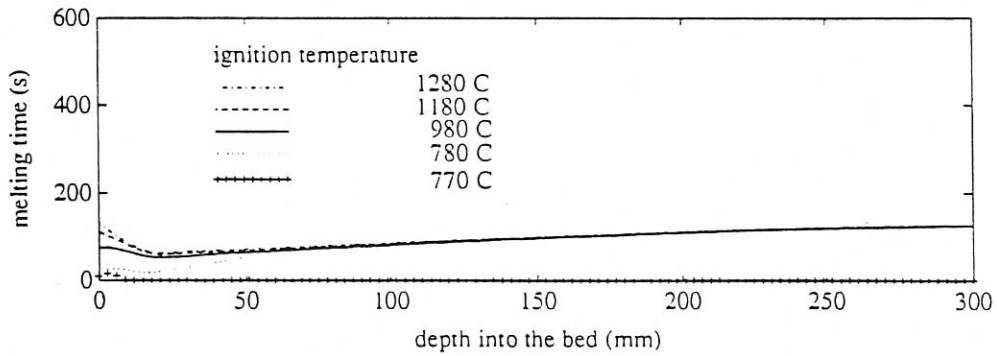

Fig. 40 Effect of Changing Ignition Temperature on Melting Time

It is indicated that a change in fan-suction affects the melting time in the same way as changing strand speed in Fig.41. If suction is too low, the lower laid mixture can not be sintered.

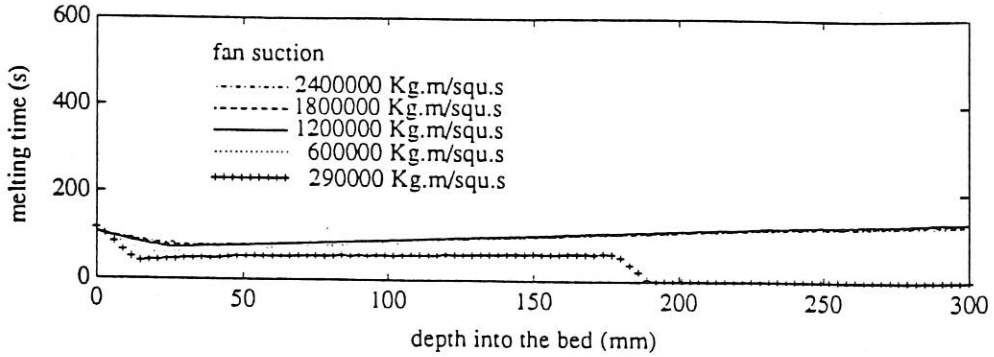

Fig. 41 Effect of Changing Fan Suction on Melting Time

The use of pre-heated air after ignition affects the melting time in such a way that the melting is improved by equalizing the melting time in a section from top to bottom, shown in Fig.42, Fig.43, Fig.44 and Fig.45. The pre-heated air drawn in reduces the need of heat for convective heat transfer between hot solid and cold air in the upper layer so the melting time is extended.

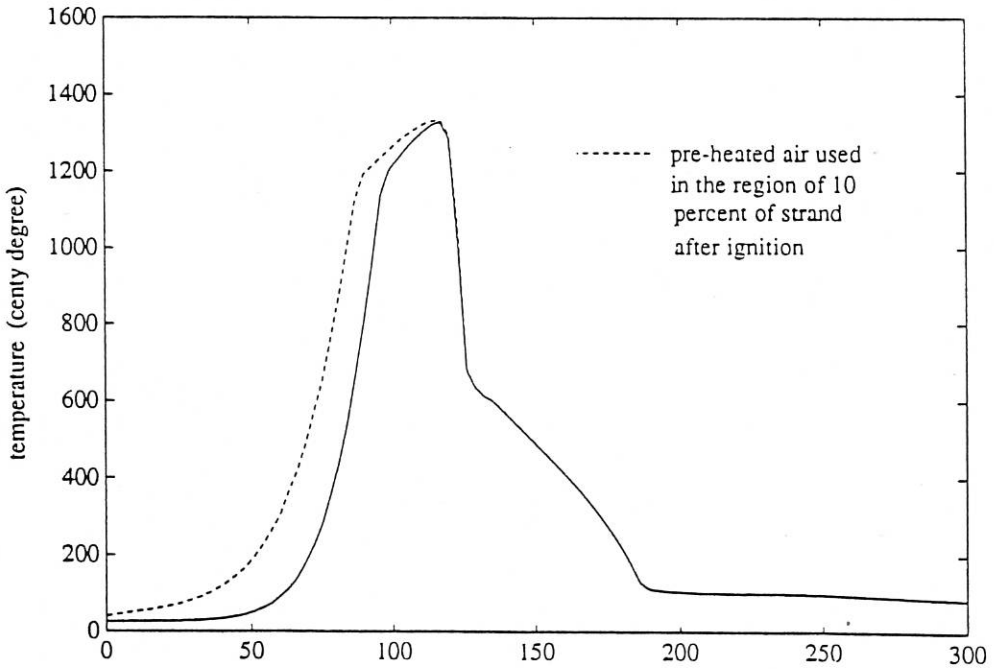

Fig. 42 Effect of Using Pre-heated Air After Ignition on Solid Temperature in a Section

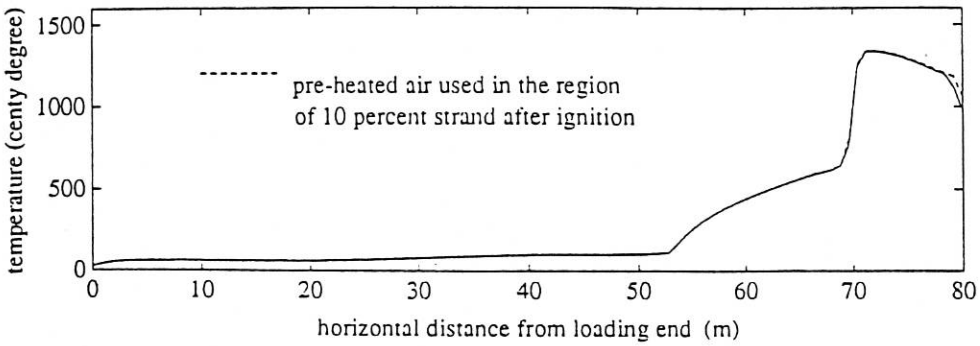

Fig. 43 Effect of Using Pre-heated Air After Ignition on Solid Temperature in a Zone

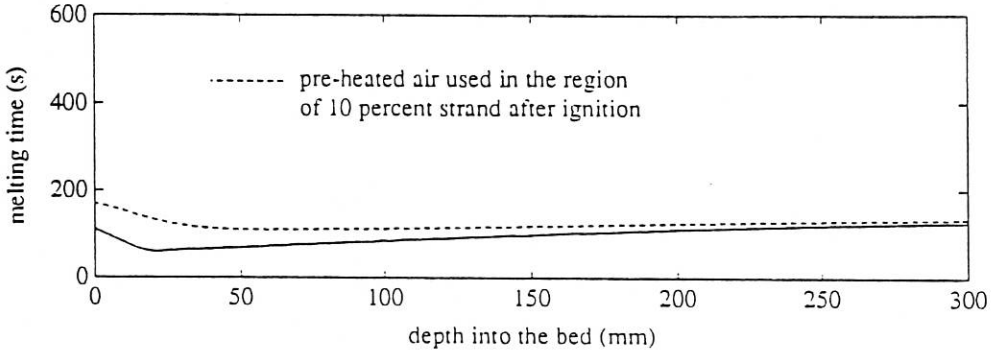

Fig. 44 Effect of Using Pre-heated Air After Ignition on Melting Time

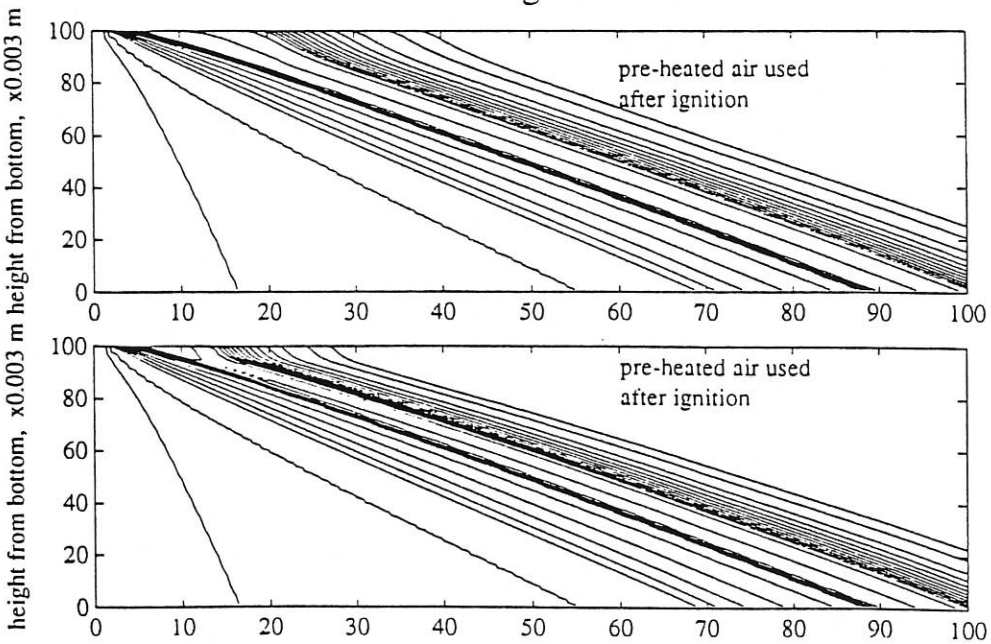

Fig. 45 Effect of Using Pre-heated Air After Ignition on Sintering Process in Bed

In fact the melting time must be assessed by the analysis of sinter quality in plant laboratory.

Chemical Composition

Changes in various operating conditions and input variables for the sintering bed do not affect the chemical composition in the sinter product except that the proportion of raw materials is changed.

Temperature and Velocity in Exhausted Gas

A change in coke-addition affects both maximium temperature and velocity of the exhausted gas. There is no significant effect on the distribution of temperature and velocity along the strand, only higher temperature and faster velocity appear earlier when the more coke addition is applied. This is shown in Fig.46 and Fig.47.

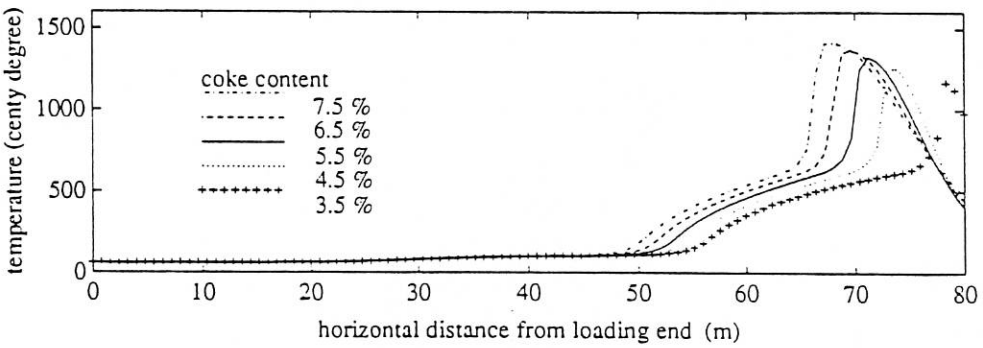

Fig. 46 Effect of Changing Coke-addition on Exhaust Gas Temperature

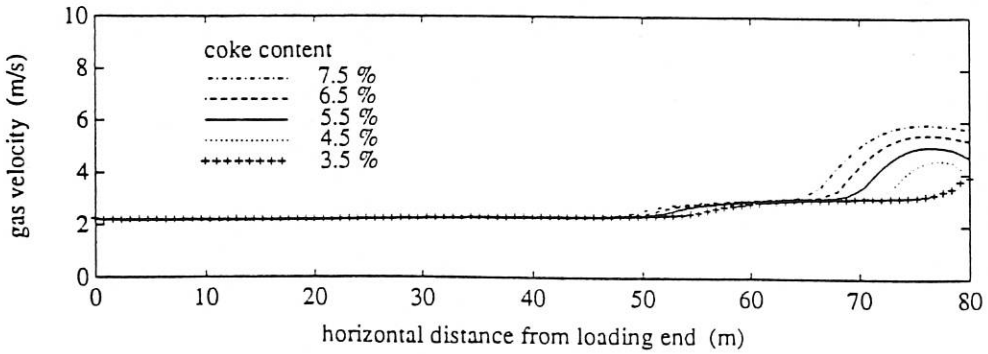

Fig. 47 Effect of Changing Coke-addition on Exhaust Gas Velocity

A change in water-addition affects the distribution of temperature and velocity in the exhausted gas. The higher the moisture content in the solid mixture, the earlier the higher temperature and faster velocity appear. Water-addition changes also affect the value of the exhausted gas velocity due to the improved permeability of bed. Fig.48 and Fig.49 show this case.

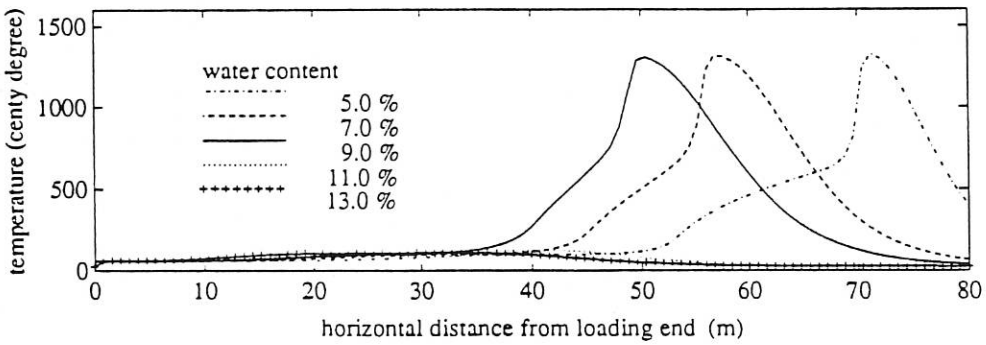

Fig. 48 Effect of Changing Water-addition on Exhaust Gas Temperature

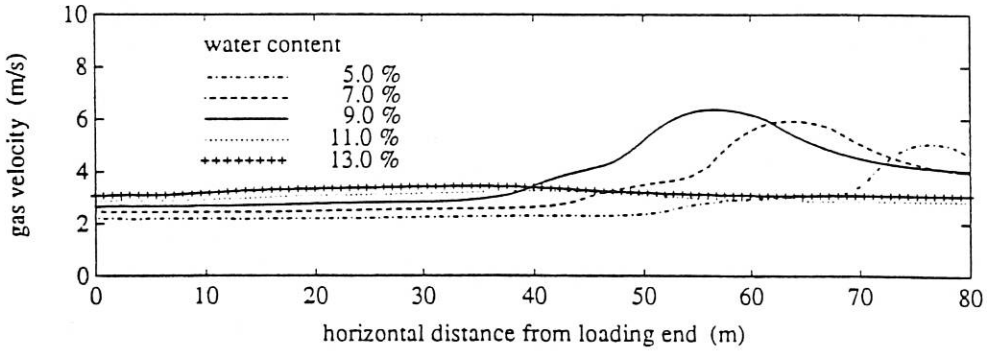

Fig. 49 Effect of Changing Water-addition on Exhaust Gas Velocity

Fig.50 and Fig.51 show that a change of limestone addition affects the distribution of temperature and velocity in the exhausted gas and the maximium value of gas velocity.

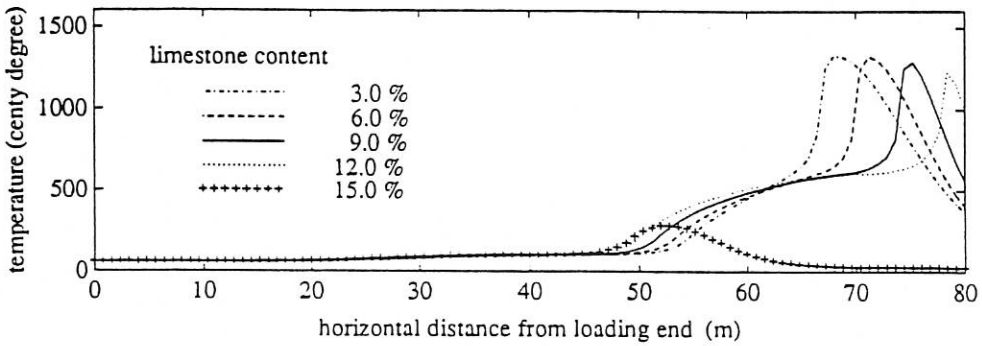

Fig. 50 Effect of Changing Limestone-addition on Exhaust Gas Temperature

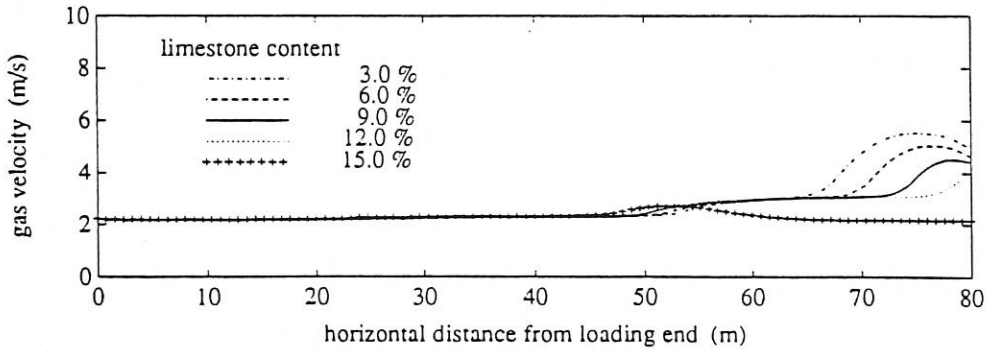

Fig. 51 Effect of Changing Limestone-addition on Exhaust Gas Velocity

A change of strand speed significantly affects the distribution of temperature and velocity in the exhausted gas, shown in Fig.52 and Fig.53. The maximium temperature and velocity occur earlier with slower strand speed.

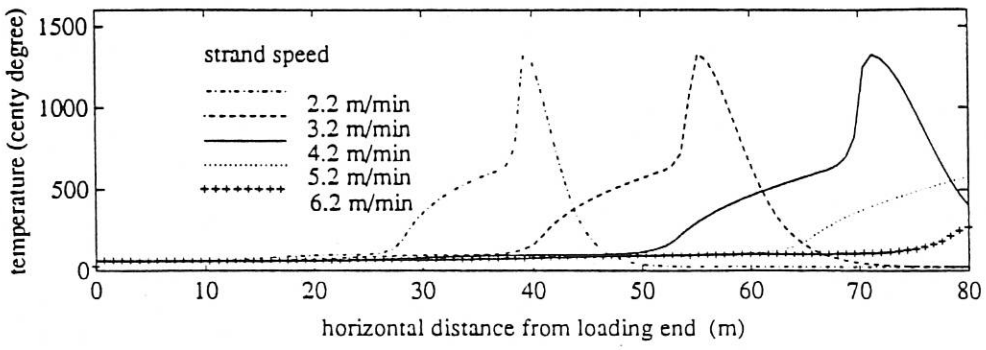

Fig. 52 Effect of Changing Strand Speed
on Exhaust Gas Temperature

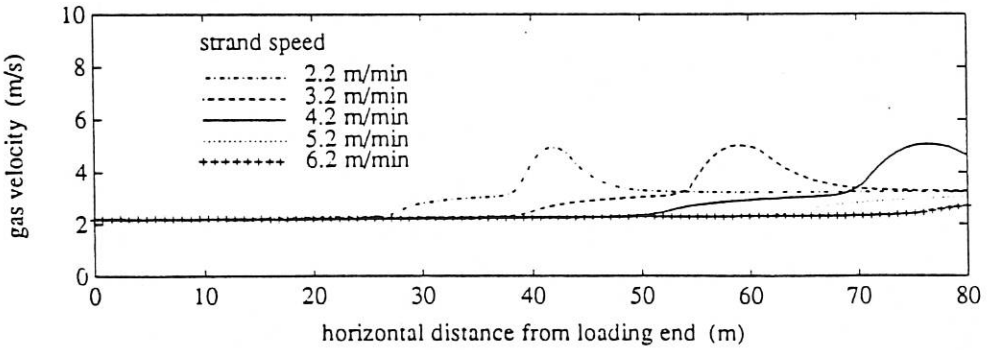

Fig. 53 Effect of Changing Strand Speed
on Exhaust Gas Velocity

A change of ignition time and temperature, also using the pre-heated air after ignition do not affect the temperature and velocity in the exhausted gas, shown in Fig.54, Fig.55, Fig.56, Fig.57, Fig.58 and Fig.59.

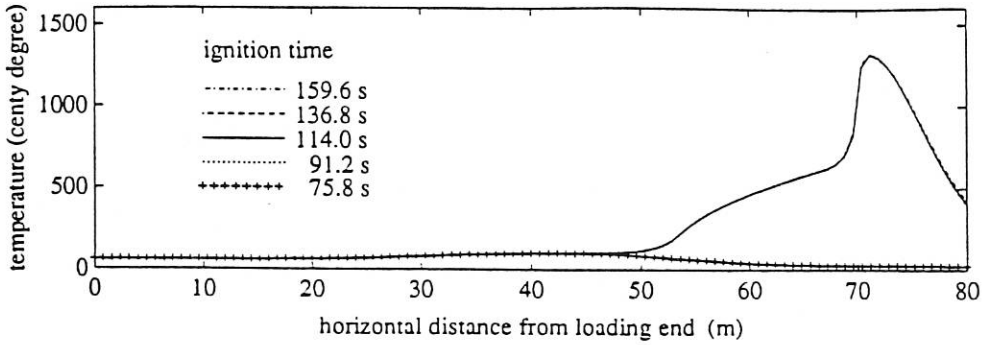

Fig. 54 Effect of Changing Ignition Time on Exhaust Gas Temperature

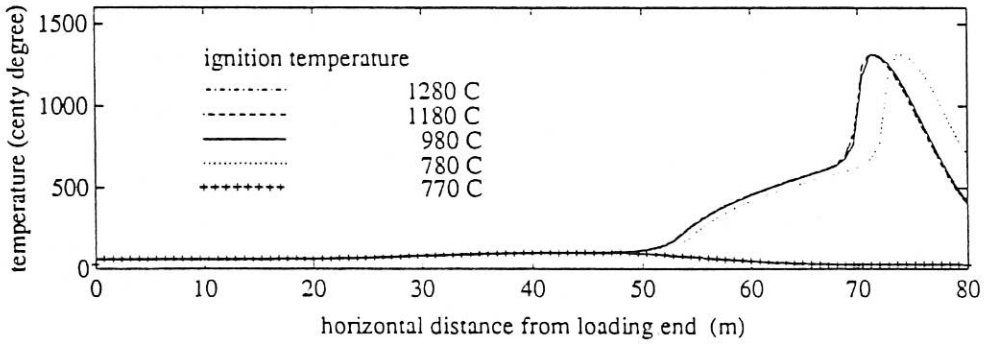

Fig. 55 Effect of Changing Ignition Temperature on Exhaust Gas Temperature

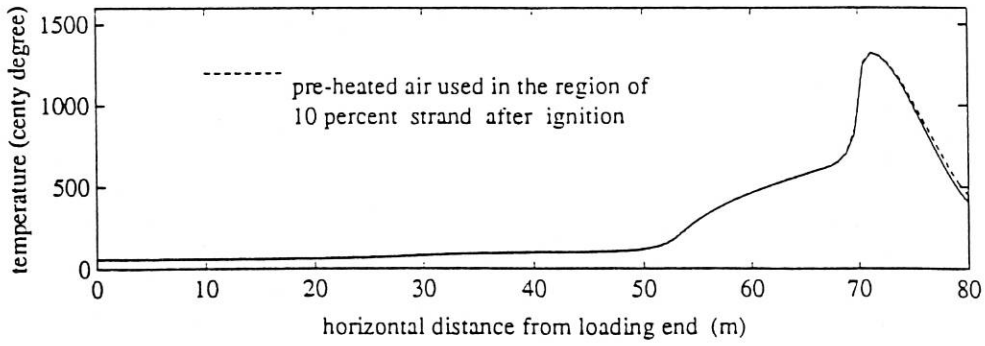

Fig. 56 Effect of Using Pre-heated Air After Ignition on Exhaust Gas Temperature

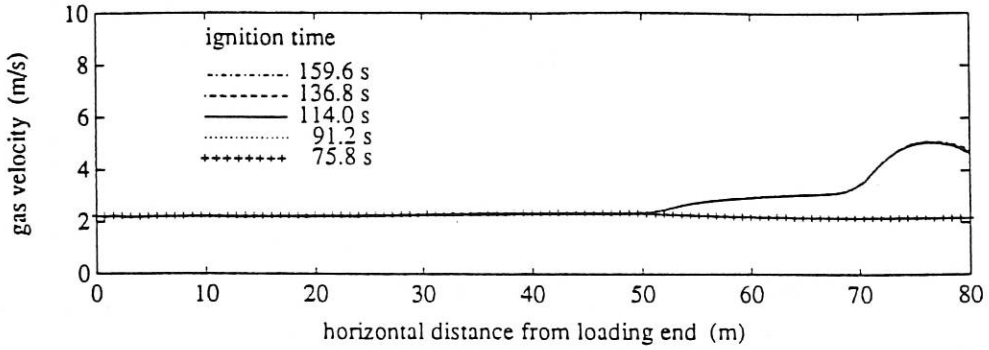

Fig. 57 Effect of Changing Ignition Time on Exhaust Gas Velocity

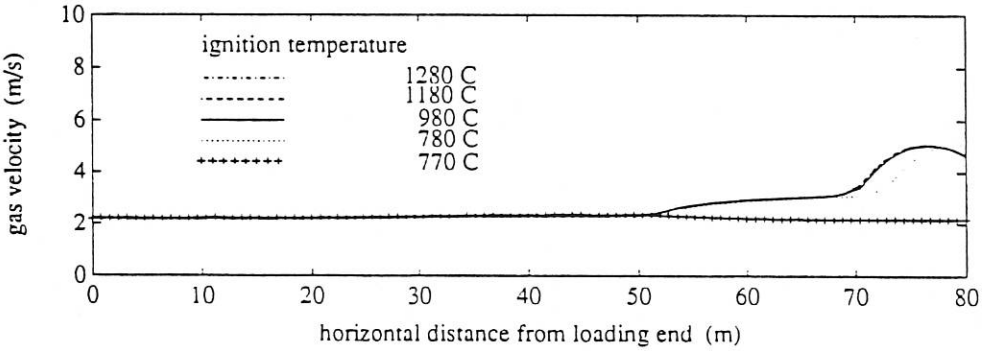

Fig. 58 Effect of Changing Ignition Temperature on Exhaust Gas Velocity

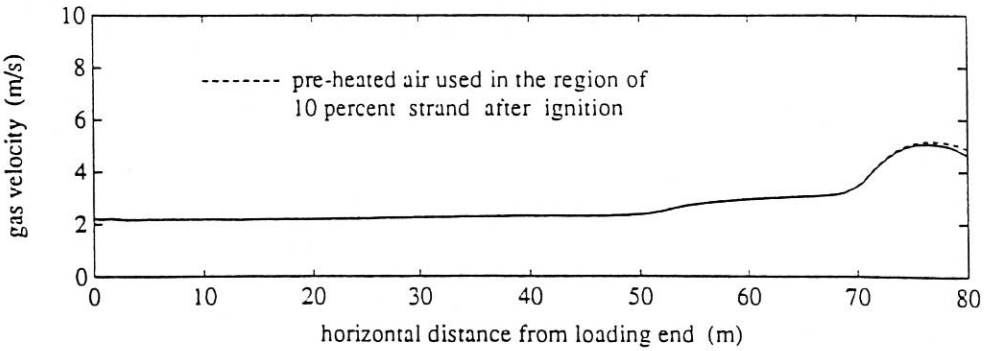

Fig. 59 Effect of Using Pre-heated Air After Ignition on Exhaust Gas Velocity

Change in fan suction affects the distribution of temperature and velocity in the exhausted gas along strand, and there is an important effect on the value of exhausted gas velocity. This is shown in Fig.60 and Fig.61.

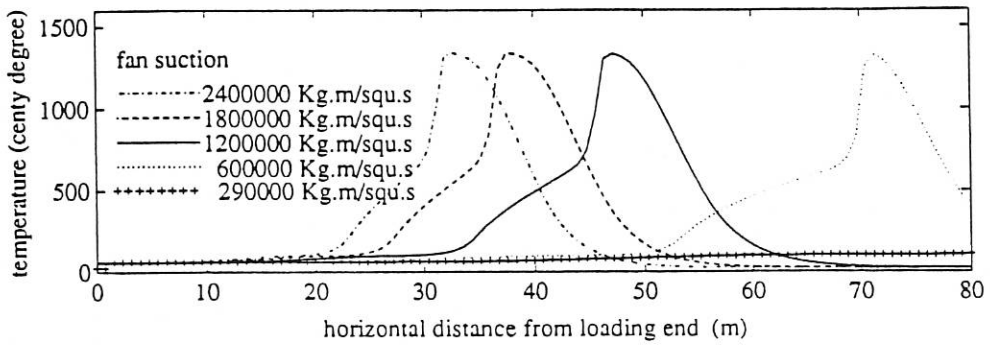

Fig. 60 Effect of Changing Fan Suction on Exhaust Gas Temperature

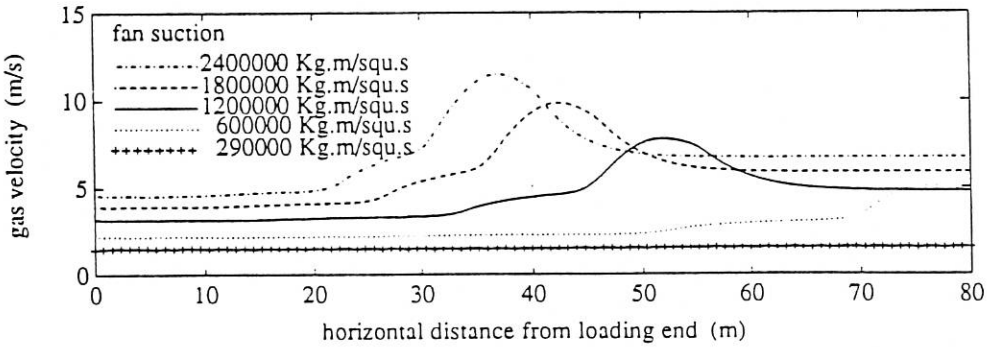

Fig. 61 Effect of Changing Fan Suction on Exhaust Gas Velocity

The observation of exhausted gas temperature or velocity can be used to determine the burnthrough position and fusion zone.

Oxygen and Carbon Dioxide Content in the Exhaust Gas

Generally the levels of oxygen and carbon dioxide content in the exhaust gas are determined by the level of coke addition, shown in Fig.62 and Fig.63.

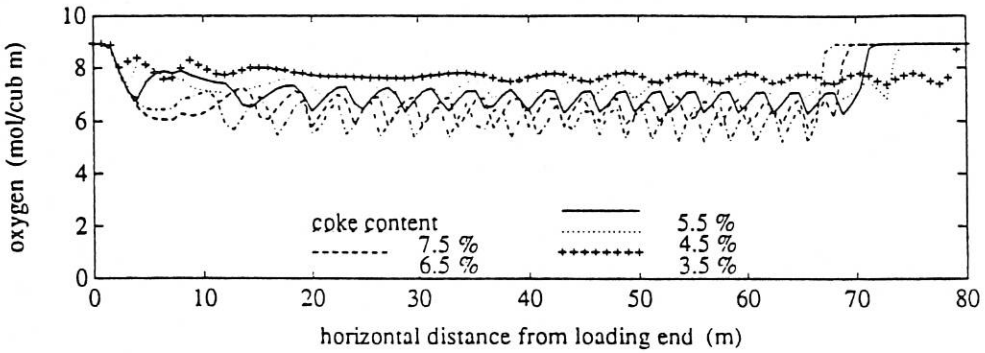

Fig. 62 Effect of Changing Coke-addition
on Oxygen Content in Exhaust Gas

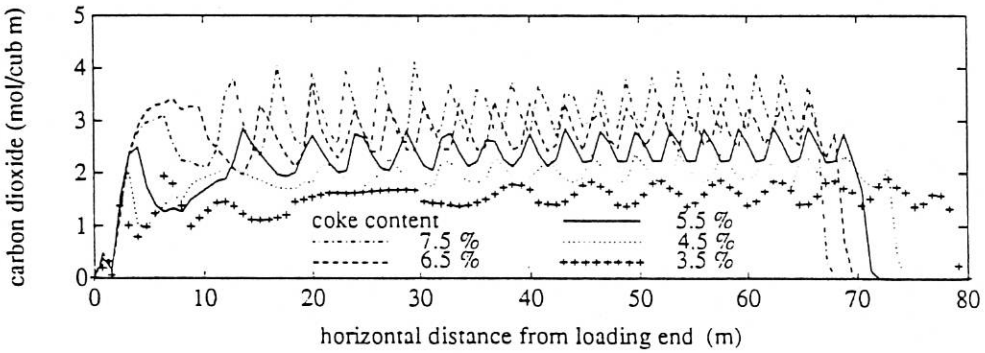

Fig. 63 Effect of Changing Coke-addition
on Carbon Dioxide Content in Exhaust Gas

The change of other operating conditions and input variables only affect the equality of oxygen and carbon dioxide content in distribution along the strand, shown in Fig.64, Fig.65, Fig.66, Fig.67, Fig.68, Fig.69, Fig.70, Fig.71, Fig.72, and Fig.73. The more equal-distribution is observed by the faster gas flow rate (gas velocity) in Fig.49, Fig.74 and Fig.75, and in Fig.61, Fig.76 and Fig.77.

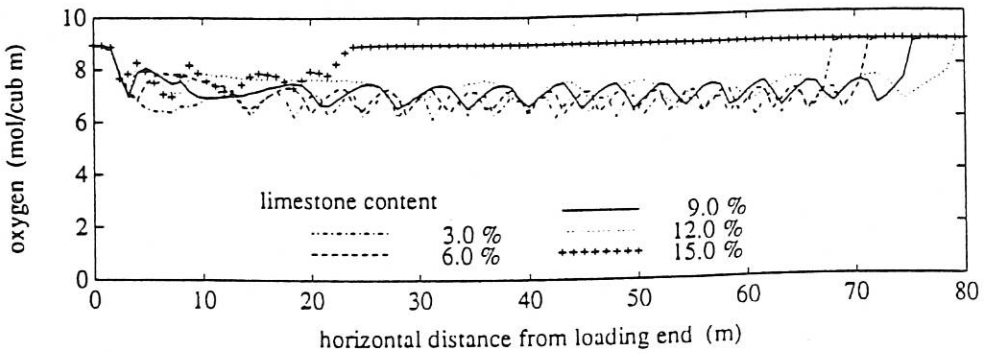

Fig. 64 Effect of Changing Limestone-addition on Oxygen Content in Exhaust Gas

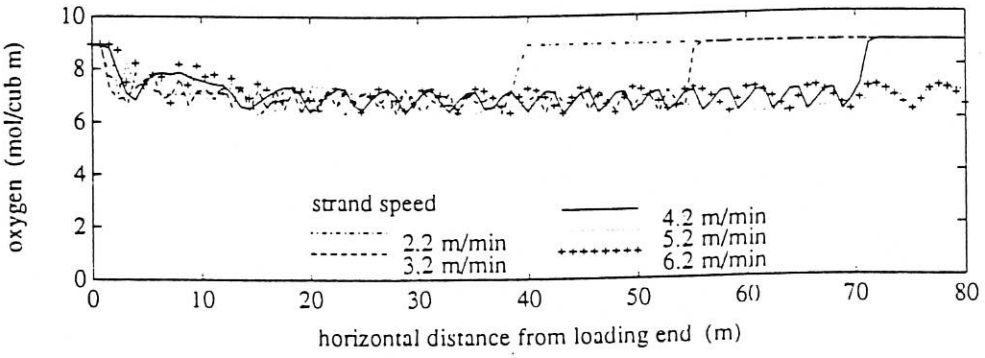

Fig. 65 Effect of Changing Strand Speed on Oxygen Content in Exhaust Gas

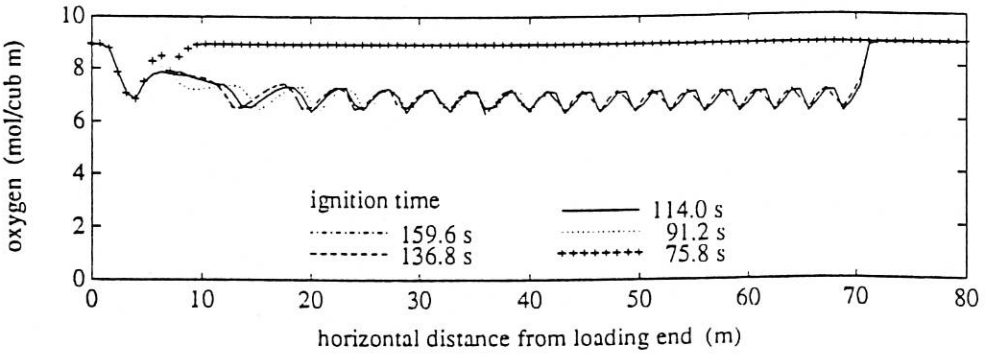

Fig. 66 Effect of Changing Ignition Time on Oxygen Content in Exhaust Gas

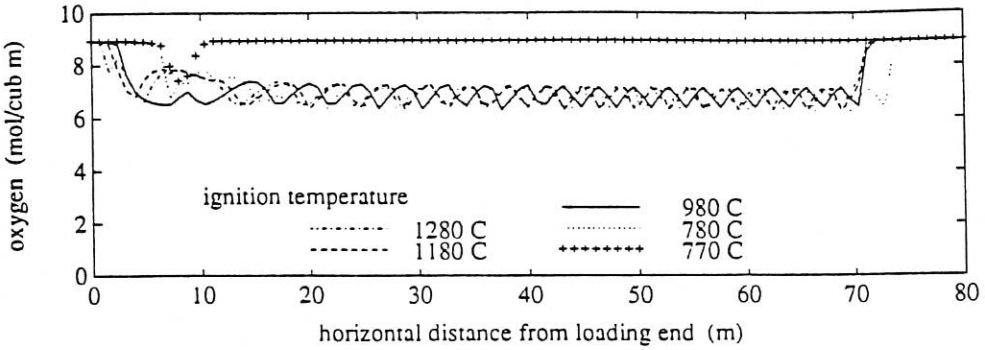

Fig. 67 Effect of Changing Ignition Temperature on Oxygen Content in Exhaust Gas

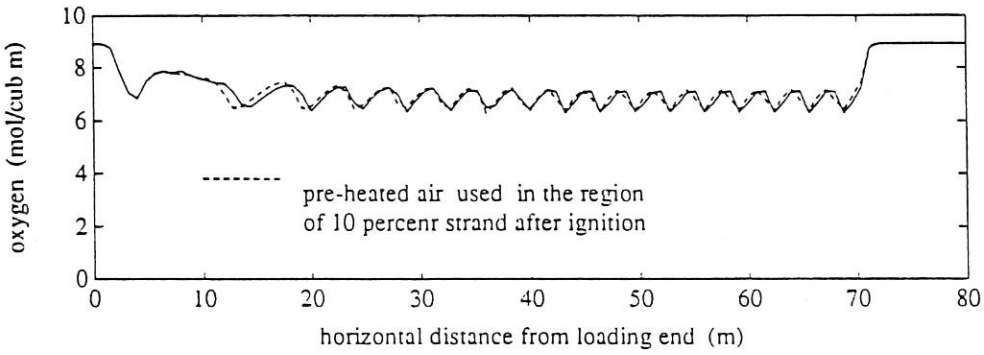

Fig. 68 Effect of Using Pre-heated Air After Ignition on Oxygen Content in Exhaust Gas

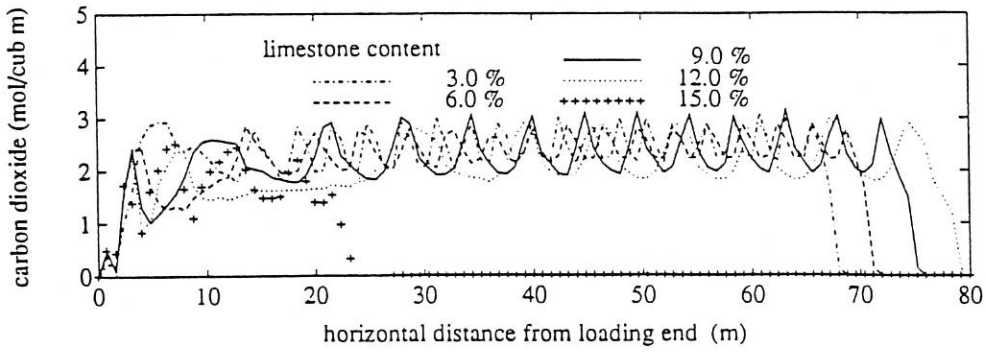

Fig. 69 Effect of Changing Limestone-addition on Carbon Dioxide Content in Exhaust Gas

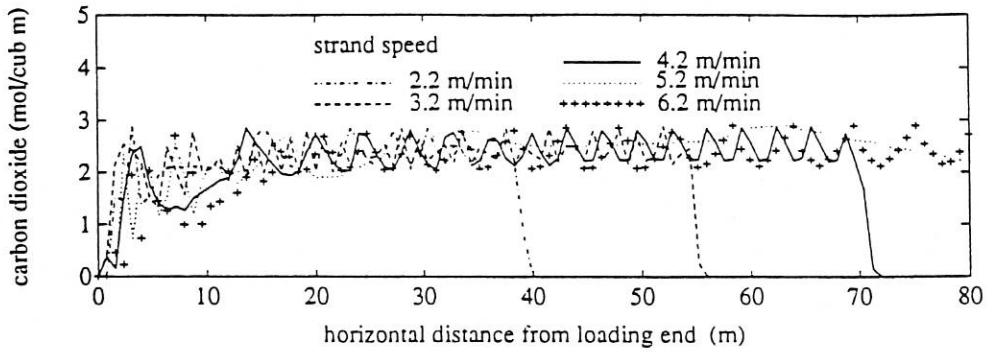

Fig. 70 Effect of Changing Strand Speed
on Carbon Dioxide Content in Exhaust Gas

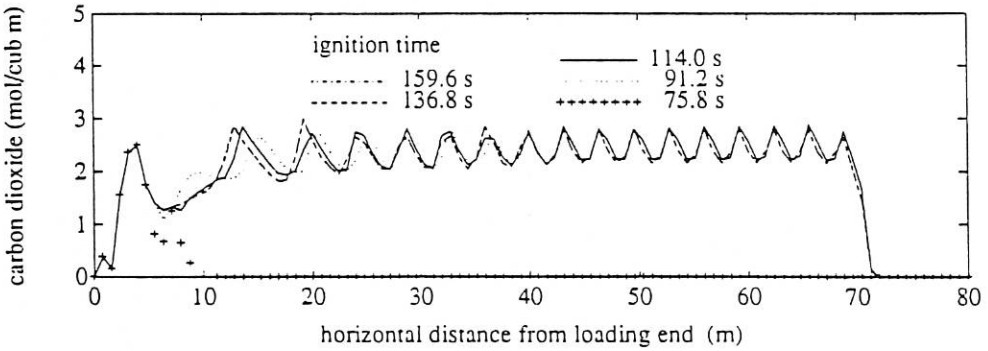

Fig. 71 Effect of Changing Ignition Time
on Carbon Dioxide Content in Exhaust Gas

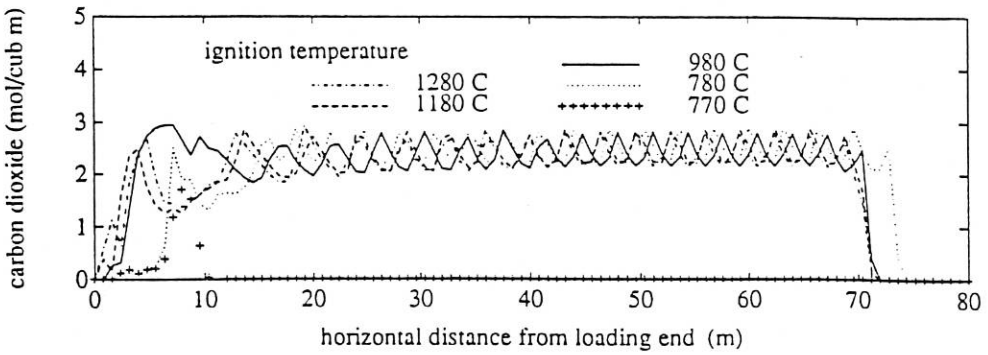

Fig. 72 Effect of Changing Ignition Temperature
on Carbon Dioxide Content in Exhaust Gas

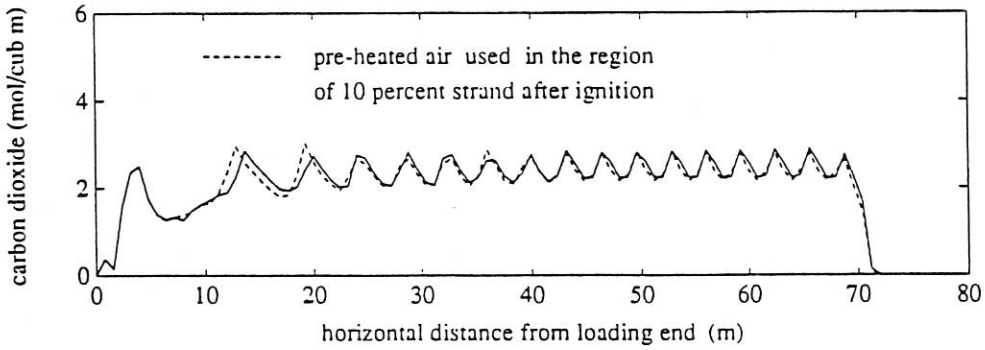

Fig. 73 Effect of Using Pre-heated Air After Ignition on Carbon Dioxide Content in Exhaust Gas

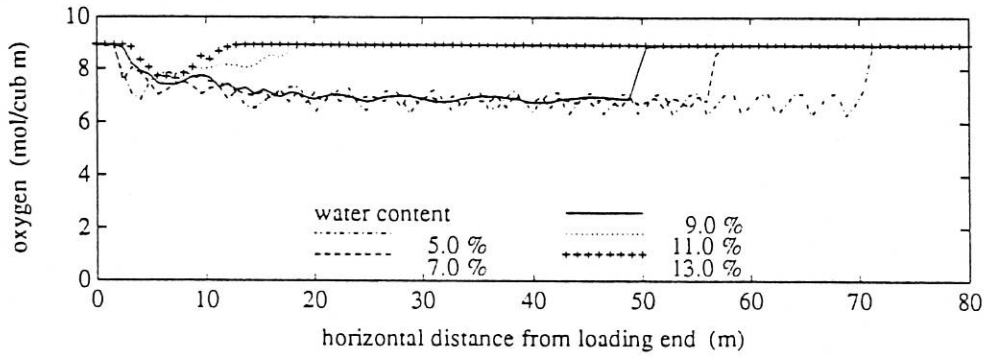

Fig. 74 Effect of Changing Water-addition on Oxygen Content in Exhaust Gas

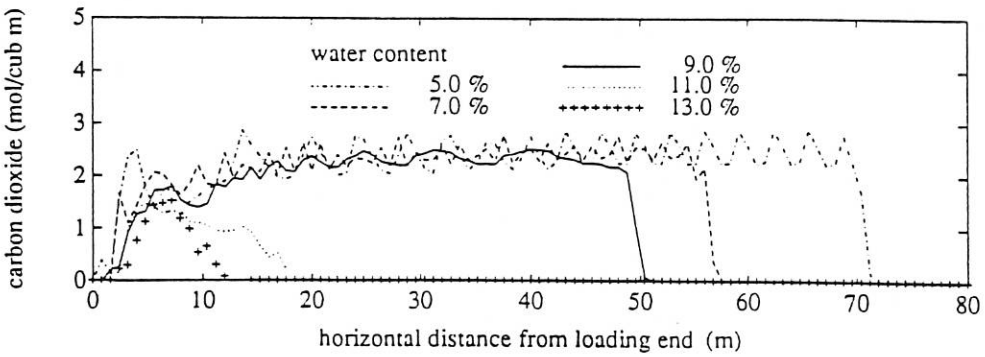

Fig. 75 Effect of Changing Water-addition on Carbon Dioxide Content in Exhaust Gas

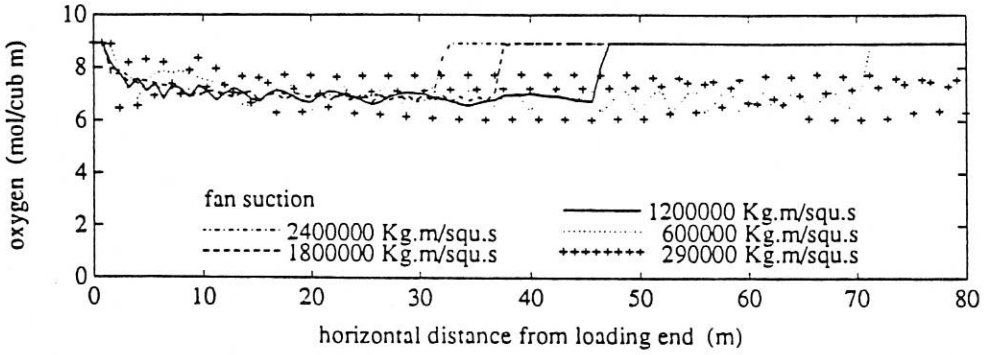

Fig. 76 Effect of Changing Fan Suction on Oxygen Content in Exhaust Gas

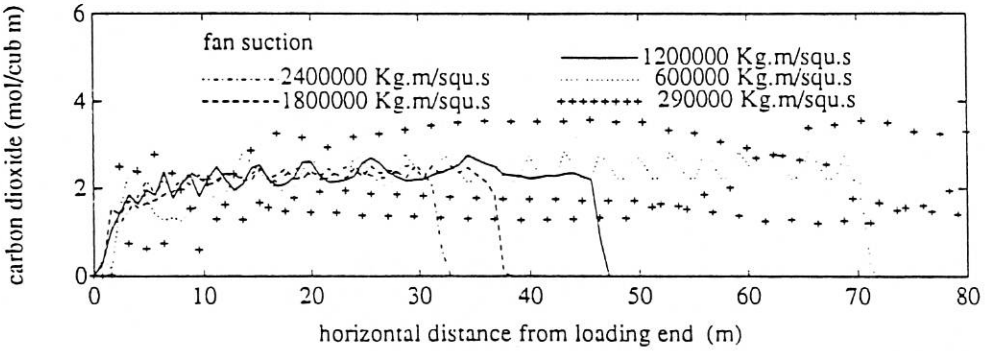

Fig. 77 Effect of Changing Fan Suction on Carbon Dioxide Content in Exhaust Gas

DYNAMICAL SIMULATION OF SINTER PLANT

A dynamical simulation model is desired when investigating the automatic control strategies, which should be a representation of the real process. The main features of the process and the relationships between the variables should be faithfully represented and the concerned information must be obtained from such a simulation model.

It is very time consuming to run a digital simulation for a complex dynamical process. This is the case when simulating the sinter plant because of the complexity of relationship between variables and the high parallelism involved in this process. The big difference exists between the time the real process takes to move forward through a section and the time the simulation takes to calculate the reactions in the real process, so it is

difficult to consider all process states in a dynamically simulated sinter plant.

In fact, all computer simulations are based on the discrete time approach. On the other hand, the realization of control strategies does not require all information from the process; this allows us to neglect the changes in some process states.

In the static simulation described previously it is assumed that all operating conditions and input variables are kept constant in the period taken for the solid mixture to travel from the loading end to unloading end of the strand. The result of simulation represents a static state of the process. Based on the static simulation method for the sinter plant a dynamical simulation approach is proposed so that the change of various operating conditions and input variables can be manipulated; dynamics of some process states can be continuously calculated in discrete time. Fig. 78 shows this approach.

The whole bed is still to be divided into m sections along the strand, but less sections are selected in the equal interval as the specified section from which the information of process states is collected. Suppose that there are k sections to be selected in the interval ΔL, the first section and the last section must be selected as the specified section among all m sections to ensure that the initial and final state of bed are obtained from simulation, then the solid mixture in the $(k-1)^{th}$ section will move forward to the k^{th} section in the time interval ΔT ($\Delta T = \Delta L / v$).

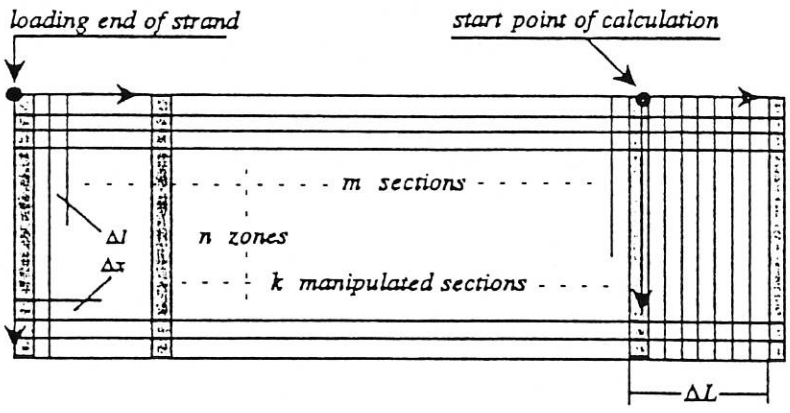

Fig. 78 Solution in dynamical Simulation

The variation of all process states involved in the model from $(k-1)^{th}$ section to k^{th} section are calculated by the same procedure as in the static simulation to ensure calculation accuracy, but the calculation is begun at

the last section (i.e the k^{th} section) backward to the loading end of bed. This means that the calculation of the process state at each point in the bed proceeds piecewise for the whole bed. In this way the variation of process states is traced in the acceptable time interval and less information is lost when any operating condition or input variable is changed.

CONCLUSION AND DISCUSSION

A basic simulation model of an iron ore sinter plant has been developed, together with appropriate techniques for its solution, these are combined in the simulation program. The main feature of the sinter plant has been taken into account in this model. The process state can be calculated at any point in the bed during a sintering operation, and the effect of changing operating conditions and input variables on the process state can be studied by this simulation model. A dynamical simulation approach is proposed so that the simulation model can be run continuously in an acceptable calculation time. This simulation model and method for its solution will be used as a basis for investigating a detailed dynamic simulation model and an appropriate control model which will be suitable for the study of automatic control srategies.

The simulation has been run with data gathered from previously presented papers. The following is a brief discussion on the model and simulation.

1. Voidage of bed

The voidage of the bed ε is an important parameter, particularly for the description of the gas flow, and is difficult to determine. It is a function of charging and height of bed and related to the different zones. It is not directly known initially, and varies locally with the position in the bed during sintering. The latter change is difficult to describe and there is presently no theoretical model available from which it can be calculated. In an ideal case the initial voidage of the bed is in the range 0.27 to 0.47, and the value of voidage varies during sintering. In this report the voidage of the bed ε is assumed to remain constant at the value 0.4.

2. Initial mean pellet diameter

The initial mean pellet diameter is related to the physical property of raw materials, water addition and stay time in the mixing drum. Normally the same raw materials are used in a certain plant for a long period, the physical property is considered to be nearly constant. Because there is no data available for accessing the relation of the initial pellet diameter and water addition at this moment, a linear equation (equ. 6) is adopted to formulate

this relation.

3. Increase of mean pellet diameter

The mechanism of mean pellet diameter increasing is complex during sintering. which is related to the physicochemical property of mixture, melting temperature, melting heat obtained by solid mixture and melting time. In this report a simplified linear equation is used to describe the mean pellet diameter increasing. The value of the increasing rate is adjusted in accordance with the initial mean pellet diameter, the final mean pellet diameter and average melting time.

4. Calculation time

The simulation algorithm is programmed currently in serial C language on SUN workstation. It takes about 70s to simulate the sintering process moving forward through a section, because there are $m \times n$ points to be calculated by using equ.(47) to equ.(87), which is quite a time consuming task. For static simulation the process states which have already be calculated remain constant when the bed moves forward due to the operating conditions and input variables remaining constant, the repeat calculation of previous sections can be omitted, therefore the simulation for the whole bed can be completed in this time interval. For dynamical simulation fewer sections are simulated. The calculation for the whole bed can be carried out as well in this time period but the cost is to lose some information of the process. For continuous dynamic simulation in real-time the calculation time is the major problem that needs to be solved.

5. Transient of process

So far the sintering process is simulated for steady state operating conditions and input variables although they may be varied in observing the effect of changing them on the sintering process. This means that the operating conditions and input variables are moved to their new static values from the old ones rather than taking into account transient changes. Actually, any change of operating conditions or input variables cannot be immediately acted upon the process because the transient exists, which depends on the corresponding time delay and time constant. But transients of some operating conditions which are changed to new values from old ones, such as the change of strand speed, fan suction and the height of solid mixture on bed, is so fast that the transient may be neglected. In the real sinter plant the transient of changing the proportion of raw materials, coke addition and water addition cannot be neglected, the large time delay and time constant exist for these changes because the preparation and mixing of raw materials are necessary stages for the sinter plant. Therefore the model described in this report should be divided into two parts so that the

different performance can be treated respectively. Fig. 79 shows such a model structure for the sinter plant.

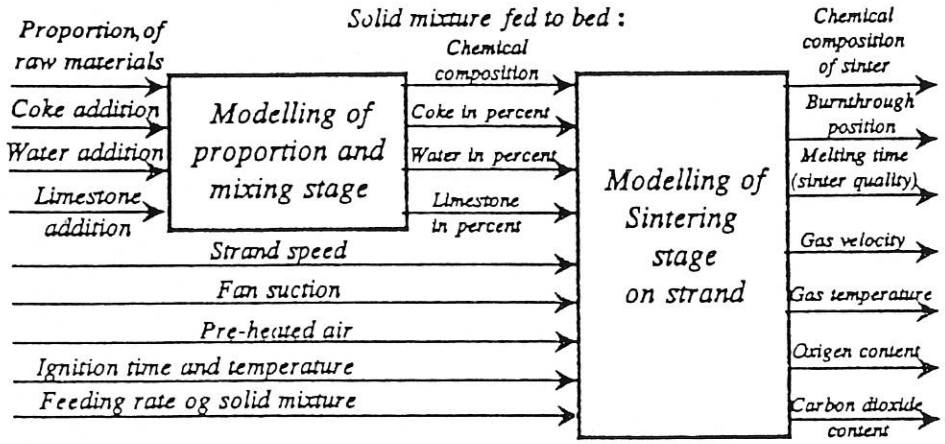

Fig. 79 Two-stage model structure on Sintering Plant

FURTHER WORK

1. The dynamical simulation approach will be improved by modelling some transients of the subprocess, such as the changes in water-addition and coke-addition, in order to produce the time response of the process outputs when changing any operating conditions or input variables. The aim is to satisfy the need of the investigation into automatic control strategies.
2. Based on the previous work the simulation model is to be transferred to the transputer facility in seeking an accomplishment of the simulation of the sinter plant by parallel distributed method in order to speed-up the calculation. There are three possible routines which can be used to decompose the simulation algorithm; decomposition according to the sub-processes involved in sintering, zone decomposition or section decomposition. A better way might be obtained from comparison of system construction, the dimension of equipment, the cost of equipment and total calculation time.
3. A control model of the studied process is necessary for high level control and fine tuning as well as the self-modification of control strategies on-line or the self-organisation of control strategies on-line. It is

difficult to establish a control model in the explicit form of a mathematical expression due to the complexity and non-linearity of the sinter plant. So a control model based on the neural network will be investigated by using the simulation model of the sinter plant.

REFERENCE

1. Ball D. F. Dartnell J. Davison J. Crieve A. and Wild R. (1973) Agglomeration of Iron Ores. *Heinemann Educational Books Limited.*
2. Rose E. (1981) Ironmaking and steelmaking - I. *Modelling of Dynamical System.* Vol.2. ed. Nicholson H. Peter Peregrinus Ltd on bchaif of the IEE. 1-43
3. Young R. W. (1977) Dynamic Mathematical Model of Sintering Process. *Ironmaking and Steelmaking.* No.6. 321-328
4. Cumming M. J. and Thurlby J. A. (1990) Development in Modelling and Sinulation of Iron Ore Sintering. *Ironmaking and Steelmaking.* Vol.17. No.4. 245-254.
5. Patisson F. Bellot J. P. Ablitzer D. Marliere E. Duley C. and Stiiler J. M. (1991) Mathematical Modelling of Iron Ore Sintering Process. *Ironmakinh and Steelmaking.* Vol.18. No.2. 89-95
6. Muchi I. and Higuchi J. (1972) Theoretical Analysis of Sintering Operation. *Trans. Iron Steel Inst. JPN.* 12. 54-63
7. Tukamoto T. Shimada S. Tagnchi T. and Higuchi J. (1970) Tetsu-to-Hagane. *J. Iron Steel Inst. JPN.* 56(6). 661-670
8. Hamada T. Koitabashi T. and Okabe K. (1972). *J. Iron Steel Inst. Jpn.* 58. 1567-1578
9. Yoshinaga M. and Kubo T. (1978) Sumitomo Search. 20. 1-13
10. Kawaguchi T. Yoshinaga M. Ichidate M. Sato S. Masuda K. and Takata K. (1987). *AIME Ironmaking Conf. Proc.* 46. 99-113
11. Dash I. R. Carter C. E. and Rose E. (1974) Measurement and Control of Quality in The Steel Industry. *Proc. Symp. Institute of Measurement and Control*
12. Dash I. R. and Rose E. (1978) Sinmulation of A Sinter Strand Process. *Ironmaking and Steelmaking.* No.1. 25-31
13. Rose E. and Dash I. R. (1979). Ind. Eng. Chem. Process Des. Dev. 18. 67-72
14. Nigo S. Kimura K. Ishimiya M. Yasumoto S. Nakashima K. and Kasahara T. (1982) *J. Iron Steel Inst. JPN.* 68. 118-125
15. Kurihara J. Fukuda A. Taraka S. and Nigo S. (1983). *AIME Ironmaking Conf. Proc.* 42. 71-78
16. Toda H. and Kato K. (1984). *Trans. Iron Steel Inst. JPN.* 24.178-186
17. Kasai E. Yagi J. and Omori Y. (1984). *AIME Ironmaking Conf. Proc.* 43. 241-249
18. Kasai E. Yagi J. and Omori Y. (1985). *4th Int. Symp. on Agglomeration.* ed. Capes C. E. 777-785. Warrendale PA. Iron and Steel Society of AIME.
19. Cumming M. J. Rankin W. J. Siemon J. R. Thurlby J. A. Thornton G. J. Kowalczyk E. A. and Batterham J. (1985). *4th Int. Symp. on Agglomeration.* ed. Capes C. E. 763-776. Warrendale PA. Iron and Steel Society of AIME.
20. Parker A. S. and Hottel H. C. (1936) Combustion rate of Carbon. *Ind. & Eng. Chem.* 28. 1334.
21. Schulter R. and Bistranes G. (1962) The Combustion zone in the Iron Ore Sintering Process. *Agglomeration* book based on Int. Symp. Philadelphia. 585-640. Pub. Wiley

22. Dash I. and Rose E. (1976) An Analytical Study of Process Occurring in An Iron Ore Sinter Bed. *Proc. Second IFAC Symp. on Automation in Mining, Mineral and Metal Processing* Johannesburgh, T9B2. 1-11.

23. Sato S. Kawaguchi T. Ichidate M. and Yoshinaga M. (1986) Melting model For Iron Ore Sintering. *Trans. ISIJ*. 26(4), 282-290.

24. Anderson R. M. (1989) A Mathematical Model of The Iron Ore Sintering Process. *Report for Degree*. Dept. of Control Engineering, Univ. of Sheffield.